Frequency Response of Human Skin *in Vivo* to Mechanical Stimulation

By

Timothy Thomas Diller

B.S. Mechanical Engineering (1997)
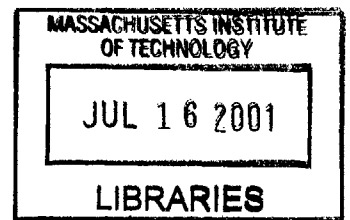The University of Texas at Austin

SUBMITTED TO THE DEPARTMENT OF MECHANICAL ENGINEERING IN
PARTIAL FULFILLMENT OF THE REQUIREMENT FOR THE DEGREE OF

MASTER OF SCIENCE IN MECHANICAL ENGINEERING
AT THE
MASSACHUSETTS INSTITUTE OF TECHNOLOGY

February 2001

BARKER

Signature of Author

Department of Mechanical Engineering
February 1, 2001

Certified by

Mandayam A. Srinivasan
Principal Research Scientist
Thesis Supervisor

Accepted by

Ain Sonin
Chairman, Graduate Committee

Frequency Response of Human Skin *in Vivo* to Mechanical Stimulation

By

Timothy Thomas, Diller

Submitted to the Department of Mechanical Engineering on
February 5, 2001 in Partial Fulfillment of the Requirements
for the Degree of Master of Science in Mechanical
Engineering

ABSTRACT

The frequency-dependent response of human skin was measured, *in vivo*, to mechanical stimulation at a scale useful in the development of tactile displays. Sinusoidal vibration stimuli of varying frequencies and amplitudes were applied with a flat-ended 0.5 mm diameter cylindrical probe under two conditions: it was either glued to the skin or not. Both normal and tangential stimlui were applied to the skin surface in the glued case and only normal stimuli were applied in the nonglued case. The stimuli were applied to live human subjects at four body sites: the finger pad, wrist, forearm, and forehead. The force-displacement response was measured and used to calculate mechanical impedance, power absorption and duty factor (an estimate of the fraction of time that the stimulator is in contact with the skin).

Results showed the mechanical impedance generally increasing in magnitude with frequency and higher in magnitude for tangential stimulation than for normal stimulation. Power absorption linearly increased with frequency, and duty factor decreased with increasing frequency and amplitude. The measured properties varied widely between body sites and subjects.

A mathematical model previously developed to calculate bulk and shear moduli from normal and tangential impedance data was tested against data at the four body sites. However, because the model assumed isotropy and semi-infinite thickness of the stimulated tissue, data taken did not fit the model well, especially at the finger tip.

Thesis Supervisor: M. A. Srinivasan
Title: Principle Research Scientist

2

ACKNOWLEDGEMENTS

TABLE OF CONTENTS

Chapter 1: Introduction

1.1. Introduction

Compared to sight and sound, the state of the art in virtual environment technology for touch is only in its beginning stages. This project is primarily motivated by the need to develop high quality tactile display devices, which would enable the user to directly touch, feel, and manipulate virtual objects. Currently, the user is limited to haptic exploration of a virtual environment through the tip of a stylus, likening the interaction to poking objects with a stick [Srinivasan & Basdogan 1997] [Srinivasan et al 1999]. To improve on this limited capability, one tactile display technology under development consists of an array of micro electro-mechanical system (MEMS) stimulators. When held in contact with a user's skin, the tactile display is designed to provide high resolution distributed-force tactile images of virtual objects.

Tactile displays of this type operate by deforming the skin at the interface site, and hence display design depends on the mechanical properties of skin. The goal of this study was to measure, *in vivo*, skin properties relevant to display design and to begin to characterize the nature of the contact at the interface in order to guide the development of future MEMS tactile displays. The current project is based on an initial study by Birch and Srinivasan [Birch 1999].

In our experiments, a cylindrical probe (representing a single MEMS stimulator) was pressed against the skin of human subjects and vibrated under various conditions. The

displacement of the probe was controlled, and the reaction force of the skin against the probe was measured. Stimuli consisted primarily of sinusoidal displacements, both normal and tangential to the surface of the skin, over a range of frequencies and amplitudes.

From these experiments we were able to measure useful mechanical properties of the skin as a function of the frequency, including mechanical impedance, and characteristics of the skin-stimulator interaction, including average power dissipation, peak contact force, and duty factor (an estimate of the fraction of time that the stimulator is in contact with the skin). A secondary goal was to calculate the frequency dependent bulk and shear moduli from the impedance data using a mathematical model of the tissue developed by De and Srinivasan [De & Srinivasan 2001]. These data and the model are intended to make possible estimation of the strain fields within the skin for arbitrary surface displacements. Strain fields play an important role in tactile perception [Srinivasan & Dandekar 1992] and such a model would be a useful tool for understanding touch and for guiding the development of tactile displays. In practice, however, the model relied on assumptions that appeared to be invalid, suggesting that the model must be revised.

1.2. Background

Research into the dynamic response of human tissue to vibratory stimuli began in the 1950's with work conducted for the United States Air Force. These studies were designed to assess the impact on humans of jet engines and other power plants with intense sound and vibratory fields. The mechanical impedance of skin was measured as a function of frequency over the range from 10 Hz to 20 kHz. The surface of the skin was vibrated using various stimulators with relatively large contact areas, on the order of 5–10 cm^2, and mechanical impedance was calculated based on observations of the propagation of surface waves. The measurements were made on the thigh and forearm, and showed that the absorption of acoustic and vibratory energy takes place primarily through propagation of

6

shear waves both in the plane of the skin surface and perpendicular to it. [Oestreicher 1950; Franke 1951; Moore 1970]

Later work by Moore and Mundie [Moore & Mundie 1972] investigated in detail the frequency dependent effects of static force, body site, probe area, and stimulation geometry on the mechanical impedance of skin. They concluded that the area of the probe and the static pressure exerted by the probe on the skin surface had a strong influence on the response of human skin to mechanical stimulation. Also, the presence of a surface surrounding the stimulator affected the measurement of mechanical properties at the forearm, but not at the fingertip or thenar eminence.

More recently, work has been done to characterize the response of the whole finger to vibratory and static stimuli [Srinivasan 1989; Srinivasan et al 1992; Pawluk & Howe 1996; Serina et al 1997]. Gulati and Srinivasan [1995; 1996] used a robotic stimulator to determine the frequency response of the human finger tip at amplitudes much higher than and frequencies much lower than those employed here. Hajian and Howe [1997] applied stimuli at the tip of an outstretched human finger and developed a second order model to determine the effective mechanical impedance at the tip. Pawluk and Howe [1999] observed the pressure distribution and shape of the contact patch of the fingertip when pressed into a flat plate in order to ascertain the large-scale response of the fingertip to indentation. Their work proposed a mathematical model based on the contact of a linear viscoelastic sphere with a rigid plane. Karason & Srinivasan [1995] employed a slightly different apparatus and modeling approach to identify the impedance parameters of the finger pad as well as finger as a whole.

1.3. Stimulation Model

In the model developed by De and Srinivasan [2001], the skin is represented by a semi-infinite half-space, and the stimulator probe that indents the skin is modeled as a cylinder. The linear elastic solution to a cylindrical punch indenting a half space has been

known since the 1930's (see Johnson 1985). Lee [1955] extended the linear elastic solution to the viscoelastic solution in the quasi-static case, using the correspondence principle. (See also Tschoegl [1989].) De and Srinivasan [2001] applied this viscoelastic solution to the finger pad, resulting in the model adopted for the present work.

Given certain critical simplifying assumptions, according to the model, the bulk and shear moduli of human finger pad tissue can be calculated from the following equations.

$$\overline{G}(s) = N(s)T(s)/4a[2N(s) - T(s)] \qquad (1)$$

$$\overline{K}(s) = N(s)T(s)[4N(s) - 3T(s)]/6a[3T(s) - 2N(s)][2N(s) - T(s)] \qquad (2)$$

$\overline{G}(s)$ is the frequency domain shear modulus; $\overline{K}(s)$ is the frequency domain bulk modulus; $N(s)$ is the ratio of force over displacement in the normal direction, or normal impedance; $T(s)$ is tangential impedance, and a is the radius of the indentor. Other material properties, such as the Young's Modulus or Poisson's Ratio, can be derived from the bulk and shear moduli.

Equations (1) and (2) depend on four key assumptions. First, the model assumes that the area of contact between the probe tip and the skin surface is constant and small (to satisfy the half-space assumption). Second, the model assumes that the probe tip stays in contact with the surface of the skin and does not slide. Third, it assumes that the material is homogeneous, isotropic, and linearly viscoelastic, as shown by Srinivasan et al [2001] and, finally, that the material is isotropic.

An important consequence of the isotropic assumption is that the magnitudes of N(s) and T(s) must be approximately the same. Specifically, from the equations one can see that $2/3 < |T(s)| / |N(s)| < 4/3$ must be true for both $|\overline{G}(s)|$ and $|\overline{K}(s)|$ to be positive, non-zero, and finite.

Chapter 2: Methods

Measurements of the frequency-dependent relationship between force and displacement of the skin were made at four body sites: the finger pad (distal phalanx) of the right middle finger, the dorsal side of the right wrist between the distal ends of the ulna and radius where a wrist-watch might be worn, the dorsal side of the upper right forearm about 5cm below the lateral epicondyle, and a point in the middle of the forehead. These were chosen as likely sites for the placement of MEMS tactile displays.

At each body site, multiple measurements were made in which the skin was stimulated by a 0.5 mm diameter cylindrical probe under the various conditions described in the section 2.4 "Stimuli." The test conditions included step indentations and sinusoidal displacements over a range of frequencies and amplitudes, with the probe either glued or not glued to the skin. In the glued tests the probe was displaced either normally or tangentially with respect to the skin surface, while in the non-glued tests only normal displacements were used.

2.1. Subjects

Five subjects were tested at each body site. Table 1 identifies which subjects were tested at which sites. Unfortunately, because of the length of the time required for the tests, the same five subjects could not be used for every body site, and only one subject (#3) was tested at all of the sites.

Subject #	Finger Pad	Wrist	Forearm	Forehead
1	X			
2	X			
3	X	X	X	X
4	X	X		
5	X	X	X	
6		X		
7		X	X	X
8			X	
9			X	
10				X
11				X
12				X

*Table 1: Summary of body sites measured for each subject*

The subjects ranged in age from 16 to 50. All of the subjects were right handed and were free of skin diseases that might affect the mechanical characteristics of the skin. None of the subjects regularly engaged in heavy manual labor or other activity that might cause them to have more than the normal thickness of callous at any of the measured body sites.
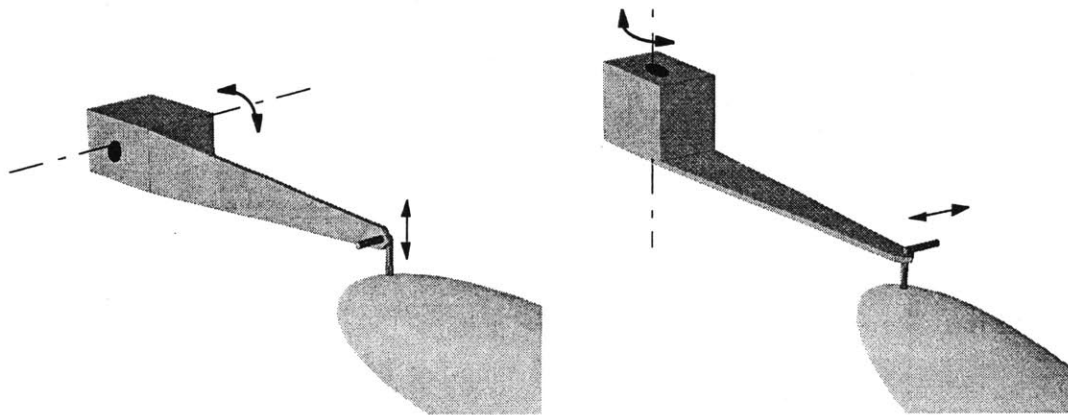
2.2. Apparatus

Measurements were made with an Aurora Scientific Model 300B Dual Mode Lever Arm System designed for use in muscle tension tests. The system comprised a brush-less permanent magnet motor and an analog electronic controller. The motor was mounted on a manual micro-positioning stage so that fine adjustments of the relative position between the motor and the subject could be made during set-up.

Figure 1 (a) shows the equipment setup in schematic form. The apparatus was controlled by a 486 based PC, equipped with a National Instruments AT-MIO-64F-5 card capable of D/A waveform generation and A/D data acquisition (DAQ) at 200 kilosamples per second with a resolution of 2.4 mV (1.2 μm and 0.12mN in the position and force channels, respectively) [National Instruments 1992]. The system provided analog signals to the controller to move the probes. For sinusoidal stimulation, a single waveform was generated in 200 discrete steps and repeated for the desired number of cycles. Similarly, for

ramp-in and ramp-out, a 200-step waveform was generated in advance and sent to the controller. The controller was tuned such that the system was roughly critically damped with a response time of 2 ms.
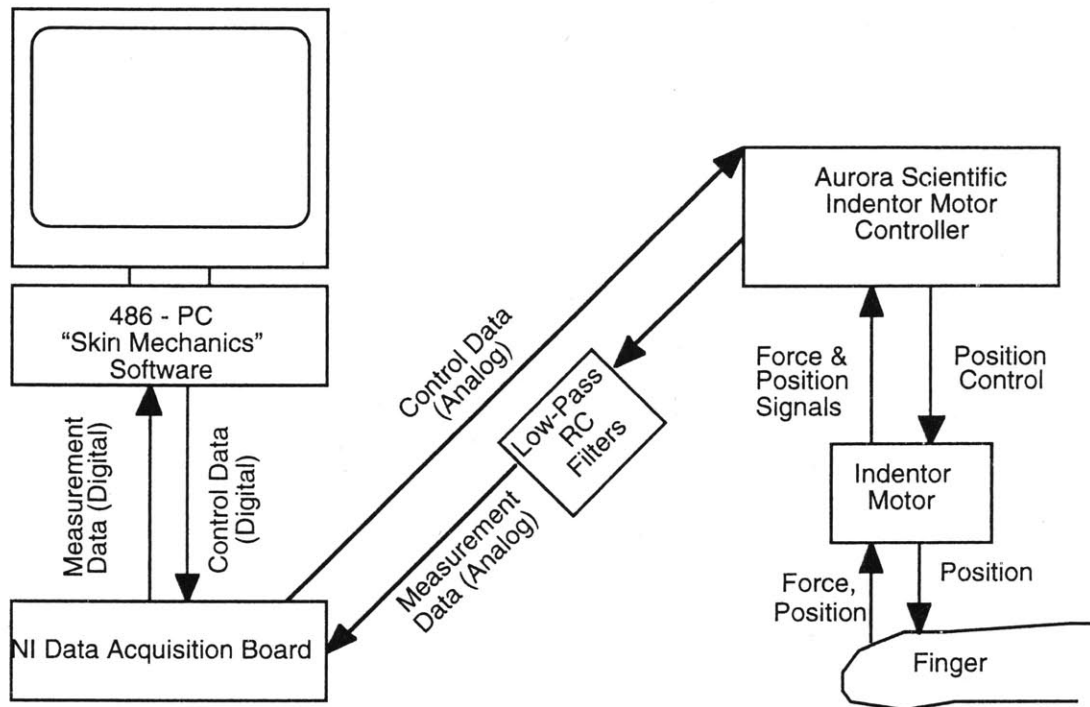
(a)

Normal Stimulation   Tangential Stimulation

(b)

Fig. 1(a) Schematic of the measurement apparatus. (b)The probe tips for normal and tangential stimulation.

Figure 1 (b) shows the arrangement of the lever arm and the two probe tips. A standard 3 cm Aurora Scientific lever arm was modified for use in the experiments by gluing two cylindrical probes to the end of the arm with epoxy. Two tips were used so that the skin surface could be displaced in either the normal or tangential direction by repositioning the apparatus. (Note that the skin was stimulated by only one tip at a time.) The tips were fashioned from 0.50 mm diameter steel wire and appeared to be good approximations of cylinders with flat tips when judged by eye under a microscope.

The maximum displacement of the operative probe tip was much less than 1 mm in the experiments, corresponding to a rotation of the lever arm of less than 0.03 radians. Consequently, the probe moved very nearly in a straight line, with motion in the off-axis direction less than 0.017 mm in a 1 mm displacement.

The Aurora controller provided analog voltage output signals corresponding to the position of the probe and the force acting on the probe. The position and force outputs were based on signals from a position sensor in the motor and the motor current, respectively. Both outputs were linear in the range of frequencies employed in the measurements. Carefully matched low-pass RC-filters with cut-off frequencies of 45 kHz were used to eliminate high-frequency electrical noise in the two outputs.

These voltage signals were read by the DAQ card during stimulation with simultaneous waveform generation. Force and position were sampled alternately at evenly spaced intervals controlled by the DAQ card, with both channels sampled at the specified sampling rate. Therefore, in each force-position pair, the times were offset by half the sampling period. During ramp-in, hold, and ramp-out, the sampling rate was 500 samples per second on each channel. During sinusoidal stimulation, the sampling rate on each channel was 40 times the stimulation frequency. Sampling data was written to a binary file at the end of each trial. Descriptive data about each trial, such as the static force, the skin surface position, and data sampling rates was written to one text file for the whole test.

12

A Polytec OFV-3001 laser doppler vibrometer (LDV) was used to gauge the performance of the apparatus. Specifically, output from the probe position sensor was compared with the position measurement of the LDV and was found to be with 1.7% agreement from 0-400Hz. The frequency response of the Aurora controller showed significant attenuation in the actual amplitude delivered to the skin between 100 and 400Hz Therefore an additional a control loop was implemented in the PC to compensate for this attenuation.

A circuit in the controller compensated for the inertia of the motor's rotor and the lever arm such that the measured force output was relatively independent of system dynamics up through 100 Hz. Resolution of the force output in this frequency range was measured to be about 0.5 mN, limited primarily by bearing friction noise in the motor. At higher frequencies, uncompensated inertial effects became more significant, reducing the force resolution to about 2mN at 200 Hz and about 6 mN at 400 Hz. This is dealt with in further detail in the section 3.3 "Analysis of Uncertainty" in Chapter 3.

2.3. Preparation of Subjects and Apparatus

When a subject arrived for a test, care was taken that at least 15 minutes passed before measurements began. This was done to ensure that measurements were made on subjects in a sedentary condition. That is, their heart rates were not above normal and their skin temperature had time to adjust to the room. During this time, subjects asked questions and read and signed informed-consent documents for "Research on Tactual Sensing and Motor Functions" in accord with application No. 1980 "For Approval to use Humans as Experimental Subjects" from the Committee on the Use of Humans as Experimental Subjects.

When measuring the finger pad, the subjects were asked to wash their hands, and when measuring the forehead, the stimulation site was swabbed lightly with alcohol to

remove any sebum or dirt. Subjects were requested not to move or talk during the test, and to hold as still as possible during the stimulation phase of each trial.

At the beginning of each test, a setup program was run to aid in moving the probe to the proper position relative to the skin surface. Since the probe was calibrated from 0 - 7.5 volts (a 3.5 mm range) with a high density of calibration points from 4 to 6 volts (a 1 mm range), the probe was positioned during setup such that stimulation occurred in the finely calibrated range. The position of the probe at the skin surface measured during setup was used as a starting point for the first trial. In each setup, the cylindrical probe was oriented by eye so that its central axis was approximately perpendicular to the surface of the skin. Hair was trimmed, shaved, or held out of the way as appropriate to prevent interference with the measurements. For every test, the static force on the probe was recorded and subtracted from subsequent measurements to eliminate the weight of the arm and probe.

In glued tests these static measurements were made just before the probe was glued. To glue the probe, a light reference mark was made on the skin surface with a fine point felt tip pen. Then a drop of ethyl cyanoacrylate (CA), or Krazy Glue™, was placed at the tip of a fine piece of wire. The wire was touched to the tip of the probe, and the probe was brought immediately into contact with the skin surface and held with light pressure for several seconds until cured. In this way, a consistent and minimal amount of glue was used, and the meniscus was kept to a minimum. If any excess glue was seen, a cotton swab moist with acetone was used to remove it before it hardened. Tests were run first in the normal direction, and after a short break the tangential test was run with the probe glued to the same reference mark as in the normal test.

During the measurements, subjects were restrained with straps to minimize the motion of the skin surface with respect to the probe reference position. In finger pad measurements, the finger nail and skin near the base of the nail and the last joint (distal interphalangial joint) were glued with CA to a stationary mount which was bolted to a table top in front of the subject, and the rest of the finger was restrained with a strap between the

14

second and third joints. The measurement apparatus was also bolted to an optical platform on the table top and was moved into position with the micro-positioning system.

For wrist measurements, the subject sat with his/her hand in a foam cradle on a table. With the palm positioned flat against the table surface, straps were tightened over the subject's forearm and hand to immobilize the wrist. The subject was then asked to relax and minimize posture change for the duration of the test. The measurement apparatus was bolted to the same optical platform on the table surface and moved into position with the micro-positioning system.

In forearm measurements, the subject sat with his/her arm resting in the same foam cradle on a table. The subject was asked to tightly grip an aluminum bar bolted perpendicularly to the platform while straps were tightened over the arm near the wrist and elbow (but at least 4cm from the measurement site). The subject was then asked to relax his/her grip and minimize posture change for the duration of the test. The measurement apparatus was positioned as with the wrist.

For forehead measurements, subjects leaned forward into two adjustable cushions, one designed to support the torso and the other designed to support the neck, face and cheeks while leaving the forehead exposed. Subjects were given straps to help support the neck and lower back. The measurement apparatus was mounted to an adjustable aluminum frame and was brought into contact with the subject's forehead after they were positioned. Tight restraint of the head and neck was not possible because of the discomfort it would cause, so subjects were asked to remain as still as possible during the measurement phase of each trial. They were trained to know when the critical DAQ portion of the trial was in progress by looking at an oscilloscope display. At the end of the test, the cushions were lightly swabbed with rubbing alcohol to remove any sebum and to disinfect the surfaces.

At the end of each glued-probe test, acetone was used to dissolve the glue at the probe-skin joint and to remove the finger from its mount in finger pad tests. The probe tip was then swabbed with acetone until all of the hardened glue was dissolved. Both probe tips

were periodically inspected to confirm that there were no scratches, glue buildup, or deformation.

2.4. Stimuli

In general, two types of stimuli were presented to the skin surface: sinusoidal stimuli and step stimuli. One combination of frequency, amplitude, and mean depth of stimulation was given in a single trial. The stimulus and response for a typical sinusoidal trial is illustrated in Figure 2. It shows the results for the finger pad of subject #4 stimulated at 1Hz with 100μm amplitude with the probe glued to the skin. See Figures A2.1-A2.11 in Appendix A for typical stimuli under other conditions. In step indentation trials, the amplitude of stimulation was set at 0 mm and otherwise had the same form as the sinusoidal trials.

Sinusoidal trials were further subdivided into two types: 1) trials with the probe glued to the skin surface and 2) trials with the probe free to lift off the skin surface. Non-glued trials were designed to simulate the interaction of a single tactile display element with the skin and were only run in the normal direction. The glued trials were designed to measure skin impedance under compressive and tensile loading in both normal and tangential directions. In addition, the data could also be used for determination of the bulk and shear moduli by ensuring that the probe remained in contact with the skin all through each sinusoidal cycle. The glued trials were further subdivided into two types: one in which the probe moved perpendicularly to the skin surface (normal stimulation) and one in which the probe moved in the plane of the skin surface (tangential stimulation.)

Trials were grouped into 'tests' according to similarity of setup and sized to accommodate the ability of the subjects to remain still (about an hour maximum). One type of test contained only non-glued sinusoidal stimuli at 400 μm preindentation; another type contained non-glued sinusoidal stimuli at 200 μm preindentation and step stimuli; a third

16

type contained glued normal stimuli and the last contained glued tangential stimuli. Each of the four test types was run on every subject at each of the body sites.
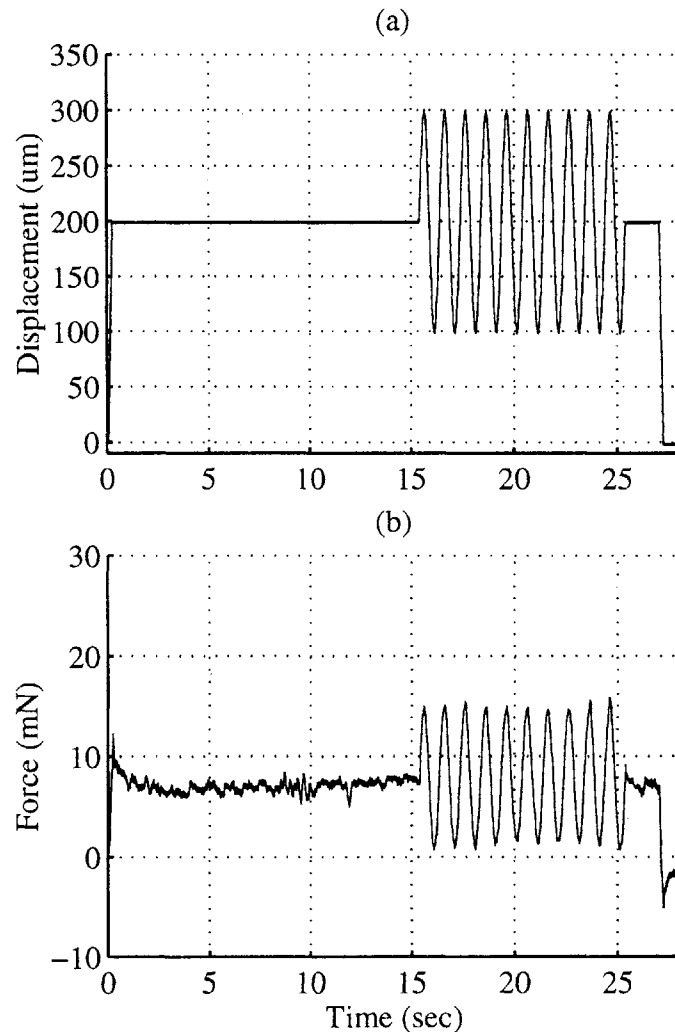

Fig. 2 - A typical stimulus and response; Stimulation is in the normal direction at 1 Hz with 100μm amplitude. Preindentation is 200μm; (a) the displacement input comprising ramp-in, hold, sinusoidal stimulation, and ramp-out; (b) the force response to the stimulation in (a) showing peak and steady-state forces and sinusoidal response.

At the beginning of each trial the probe was 'zeroed' in different ways depending on the test type. In non-glued tests, the skin surface was located at the beginning of each

trial with the probe moving 1 mm away from the last measured position of the skin surface. The probe was then moved slowly into contact with the skin until a threshold force of 3 mN was exceeded. The probe was removed 1mm from the skin surface and brought into contact three times total, and the average position was recorded as the position of the skin surface.

In glued tests, the probe was returned to a neutral force position at the start of each trial. In normal stimulation, the force on the probe in the current position was checked for sign and then moved slowly to decrease the magnitude of the measured force. Once the sign of the measured force changed, the probe position was marked as the skin surface. Again, three repetitions were averaged to obtain the actual value used. In glued tangential trials, the same zeroing procedure was used at the beginning of each trial, but since the direction of probe motion was parallel to the plane of the skin surface, the probe was returned to a neutral position, with no strain in the direction of stimulation. In this case, the preindentation depth was set by hand, using the micro-positioning system for finger pad, wrist and forearm, and estimated by eye for the forehead. In tangential trials, the probe had to be monitored by eye and, if necessary, adjusted to keep it at the same preindentation depth.

In the case of normal indentation tests, after zeroing, data acquisition began a few milliseconds before the probe was moved to the preindentation depth. This brief pause before ramping in was included to ensure that the starting point of the probe was recorded for post-processing. To pre-indent the skin, the probe was moved to the specified depth at a rate of 1 mm/sec in sinusoidal stimulation trials. In step indentation trials, the rate of indentation was 100 mm/sec to achieve a rate as near as possible to a step input. A 15 second pause after ramp-in allowed for viscoelastic recovery so that a steady state response of the skin was measured. This is visible as the exponential decay in the force in Figure 2(b). In the tangential tests, preindentation was perpendicular to the direction of stimulation and set manually, so in each no time was needed for viscoelastic recovery. During the preindentation and recovery phases of the trial, force and position were sampled at 500 samples per second.

18

In trials with stimulation frequencies of 10 Hz and higher, sinusoidal stimulation began with an amplitude control program (shown by a cut line in Figure 2). The program matched the measured stimulation amplitude with the desired stimulation amplitude to counteract the effects of attenuation in the control of the stimulator. Data acquisition was turned off during the amplitude control phase, which generally lasted no more than 2 seconds, so this phase is not apparent in any of the figures.

Once the desired amplitude was achieved it was held, and data acquisition on each channel resumed at 40 samples per stimulation cycle. After a short pause at the end of sinusoidal stimulation, the probe was retracted to the initial position, and data sampling was stopped. A pause of 30 seconds separated each trial to allow for full recovery of the skin to the undeformed state.

2.5. Test Conditions

Each test stimulating in the normal direction began with two 30-second, 100 Hz, 250µm amplitude preconditioning stimuli. Preconditioning in the tangential stimulation tests was similar, but with an amplitude of 100µm. Preconditioning trials were given to eliminate any transient stress history effects in the first measurements of the test. After the preconditioning trials, each combination of amplitude, frequency, and mean depth of indentation (see Tables 2 and 3) was repeated three times in random order throughout the test.

The same set of frequencies and amplitudes, shown in Table 2, was used in both glued normal and glued tangential tests to provide analogous measurements in each direction.

Amplitude (µm)	Frequencies (Hz)
25	1, 10, 100
50	1, 2, 4, 10, 20, 40, 100, 200, 400
100	1, 10, 100

Table 2: Glued Stimulation Parameters

The glued trials were all run at a mean stimulus depth of 200µm to reduce tensile stress on the glue connection, and the mean depth was not purposely varied in the course of these tests. This depth was computer controlled during normal stimulation, but during tangential stimulation, this depth was set by hand at the beginning of the test. Although the depth may have changed in the course of the test due to subject motion (as much as ± 300 µm at the forehead as determined by the resting skin position between two trials), according to the model, the mean depth did not have any effect on the value of the impedance properties so long as stimulation remained in the linear range. 50µm was chosen as the primary amplitude, and additional stimuli were given at 25µm and 100µm for purposes of verifying viscoelastic linearity. With two preconditioning trials and three repetitions of fifteen frequency-amplitude combinations, the glued tests contained 47 stimuli each.

Since the non-glued trials were designed to simulate the actual interaction of human tissue with a tactile display, which would not be glued into place, the amplitudes measured were generally larger than those used in the glued probe tests. Additionally, since there was not the constraint of maintaining a sometimes tenuous glue connection, larger forces could be measured, reducing the percentage uncertainty. Table 3 summarizes the frequency-amplitude combinations used.

Amplitude (μm)	Frequencies (Hz)
50	1, 2, 10, 20, 100, 200
100	1, 2, 4, 10, 20, 40, 100, 200, 400
150	1, 10, 100

Table 3: Non-Glued Stimulation Parameters

All three amplitudes were measured at 1, 10, and 100 Hz in order to check the linearity of the measured range. At 2, 20, and 200 Hz, 50 μm amplitude stimuli were added to provide overlap conditions with the glued probe measurements. At 4, 40, and 400 Hz, only the primary amplitude of 100μm was run. Two preindentation depths were used for each of the amplitude-frequency combinations, 200μm in one test and 400μm in the other. Included in the 400μm preindentation tests were step stimuli with step sizes of 100, 200, 300, 400, and 500μm.

Chapter 3: Results

The displacements and the forces shown in all figures are relative to the corresponding values when the probe was barely touching the skin surface. The initial position of the probe at the skin surface has been subtracted from the signal values so that all displacements are measured relative to the starting position of the probe immediately before ramp-in. Similarly for the force measurements, the static force on the probe was measured in each setup with the probe near its operating position but not touching the skin surface. This static force of the weight of the probe lever arm and tip was subtracted from the force signal.

Figure 3 shows an example of force plotted as a function of probe position for a typical trial stimulating the finger pad with the probe either glued (a) or non-glued (b). See Figures A3.1-A3.3 in Appendix A for similar plots of data taken at the other body sites. Linear relationship during ramp indentation, viscoelastic relaxation, energy dissipation due to hysteresis, and cratering of the skin surface are all evident. In Figure 3 (a) and (b), at the beginning of a trial, while the probe is resting at the skin surface, the force varies between about 0-2 mN. During ramp in, the force increases almost linearly to about 15 mN. A short vertical line where position is constant and the force decreases is due to viscoelastic stress relaxation. The steady state force values (about 5mN in (a) and 4.8 mN in (b)) are different because of small motions by the subject. Sinusoidal stimulation produces an elliptical curve in (a), with the path in time traveling clockwise. The peak forces in (a) and (b) are

significantly different because of the differences in the type of stimulation. Probe ramp out causes a line parallel to the indentation in (a) with a force reduction of about 10 mN. The depth of crater formed by the indentation and stimulation is given by the intersection of the ramp-out line and the displacement axis (about 120 μm in (a) and 180 μm in (b)). At the end of ramp-out in glued trials the force is negative indicating tensile loading of the skin, and the final viscoelastic relaxation recovery is evident in a short vertical line to the origin. In non-glued trials, the force remains at zero as the probe lifts off the skin surface (at about 180 μm displacement) to return to the original position. It should be noted that data for the amplitude control phase, immediately prior to the sinusoidal stimulation, and the 30-second period to allow for complete strain recovery between trials was not saved by the apparatus and, hence, is not included in the figure. Whereas the steady state forces differ between the two plots due to slight subject motion after ramp-in, peak forces are substantially different due to type of stimulation.

In the following sections, results for glued and non-glued tests are reported separately. In glued trials, results include the mechanical impedance, a comparison of impedance magnitude among body sites, subjects, and probe orientations, and the bulk and shear moduli as functions of frequency. Non-glued results characterize the interaction of a tactile stimulator with the skin and substrate and include power dissipation with respect to frequency, the duty factor of the stimulator as a function of frequency and amplitude, and a summary of the force response of the skin to step indentation. Power requirements, peak and steady forces, and duty factor all have a direct impact on the design of tactile displays.

24
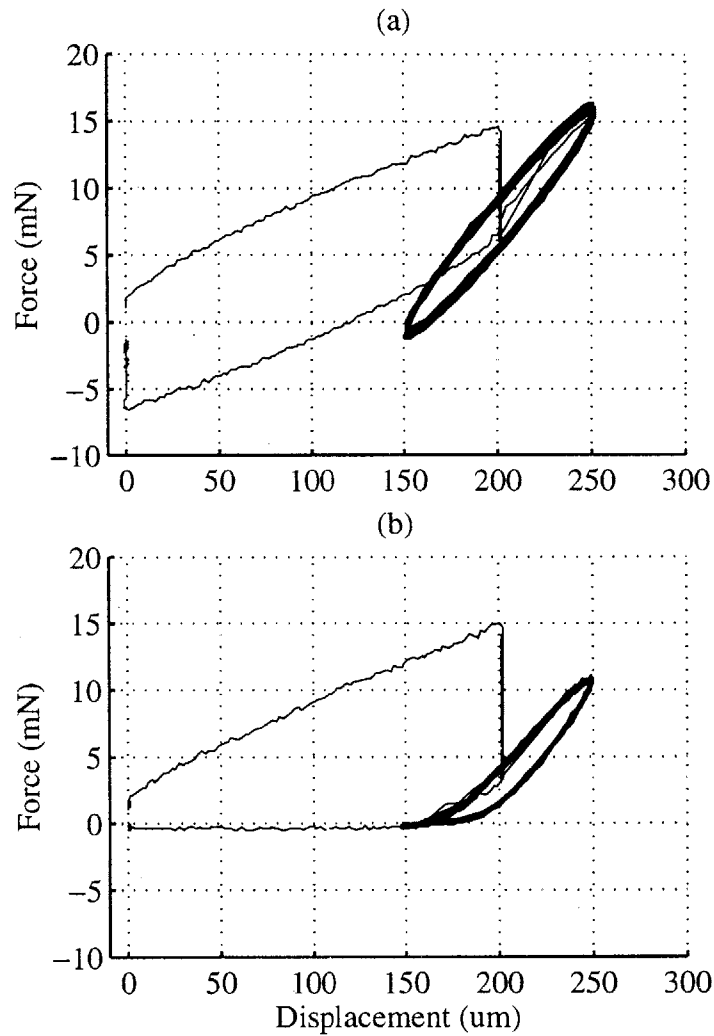
Fig. 3 - Force v. Position for the finger pad under stimulation in the normal direction at 100 Hz and 50µm amplitude with (a) the probe glued and (b) the probe not glued. Both plots show results from subject #4 under similar test conditions. These plots show ramp-in, hold, ten seconds of sinusoidal stimulation, and ramp-out.

3.1. Glued Tests

Figure 4 shows the magnitude and phase of the impedance for normal and tangential stimulation at each of the four body sites measured: (a) the finger pad, (b) the wrist, (c) the forearm, and (d) the forehead. The impedance was compiled from the complete set of stimuli over the range of frequencies for glued trials and averaged across subjects. Because stimulation was in the linear range, the amplitude of stimulation did not affect the impedance. The impedances were averaged first across all amplitudes and repetitions and then across all subjects at each frequency for plotting. See Figures A4.1 – A4.40 in Appendix A for impedance curve of every subject for each body site.
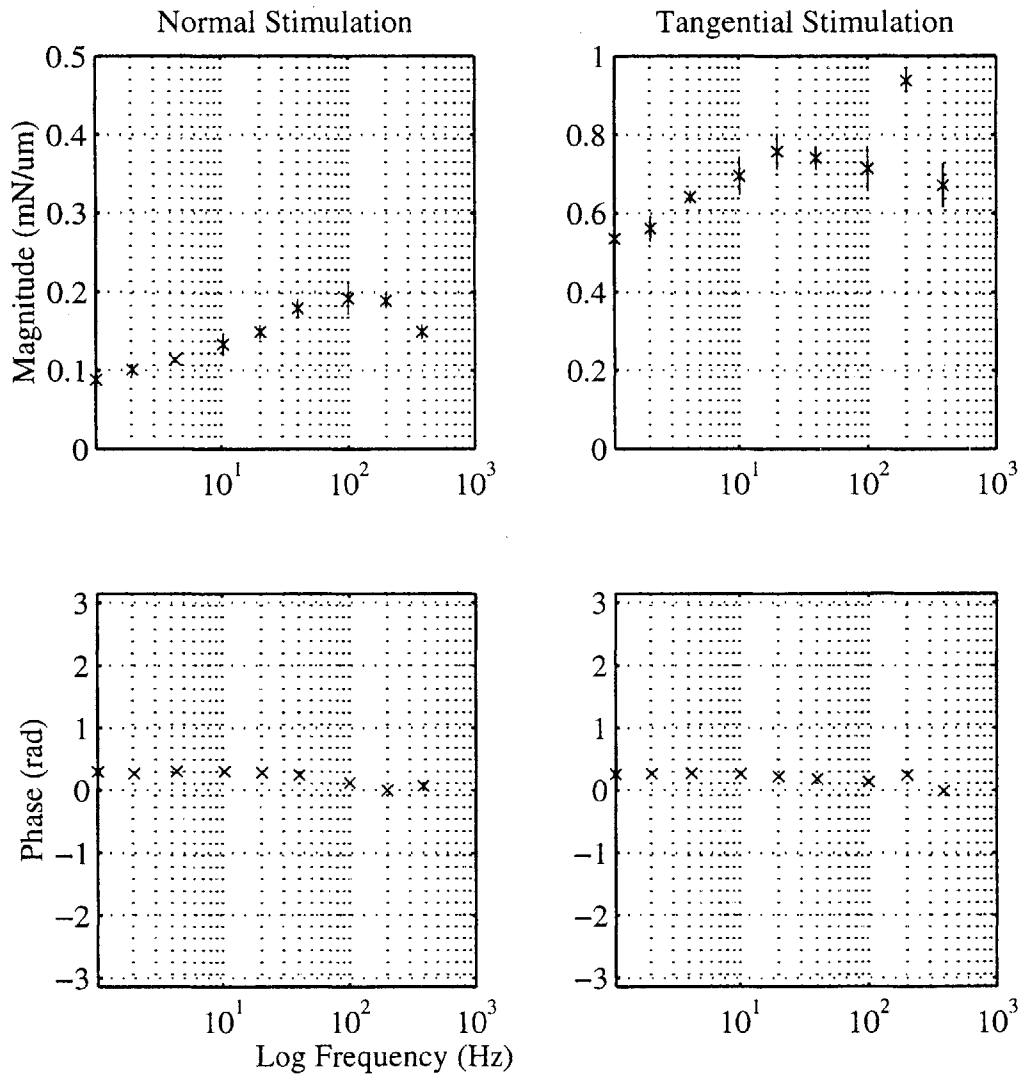
Fig. 4(a) - Impedance magnitude and phase at the finger pad for normal
and tangential stimulation. The plots show the impedance averaged
over five subjects at each body site. Error bars show standard
deviation across subjects.
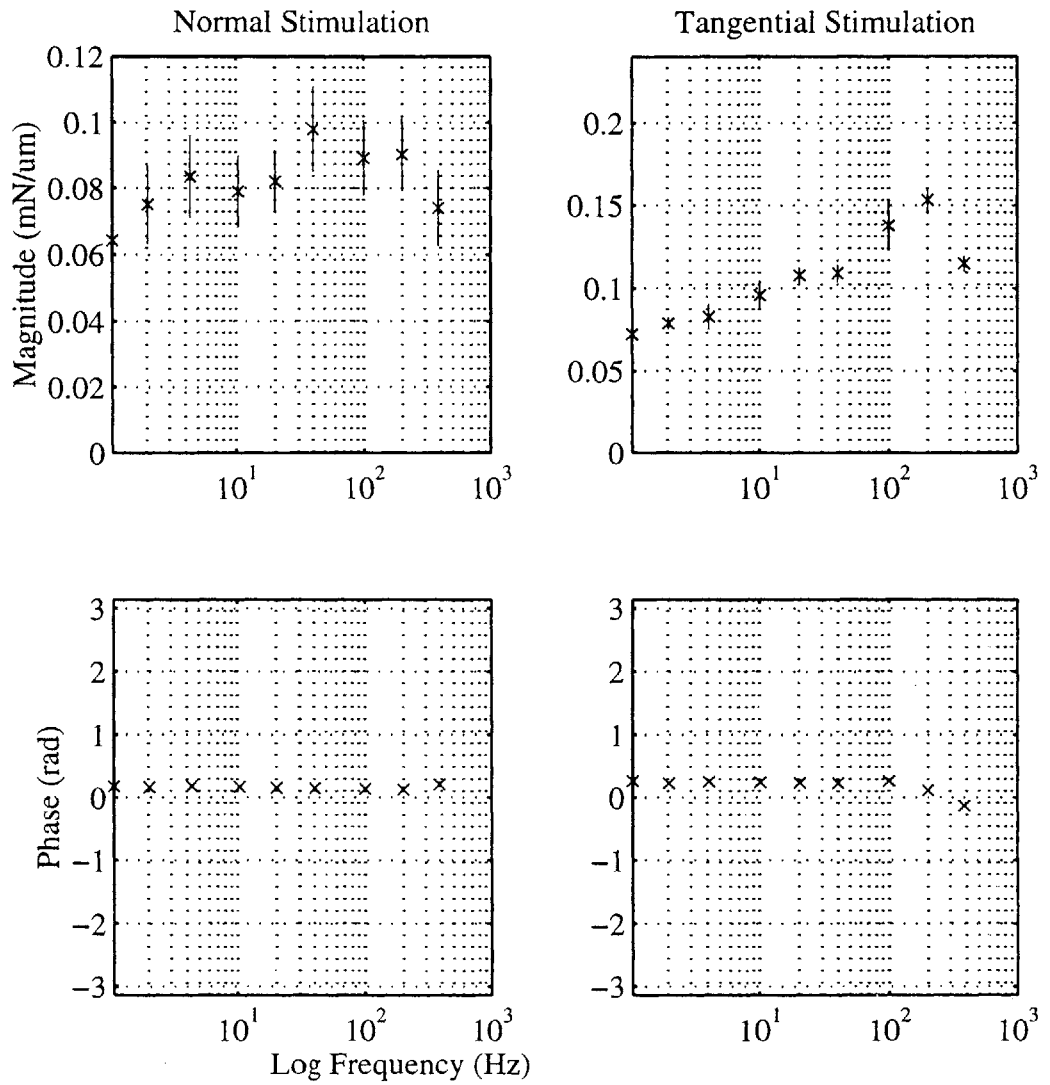
Fig. 4(b) - Impedance magnitude and phase at the wrist for normal and tangential stimulation. The plots show the impedance averaged over five subjects at each body site. Error bars show standard deviation across subjects.

28
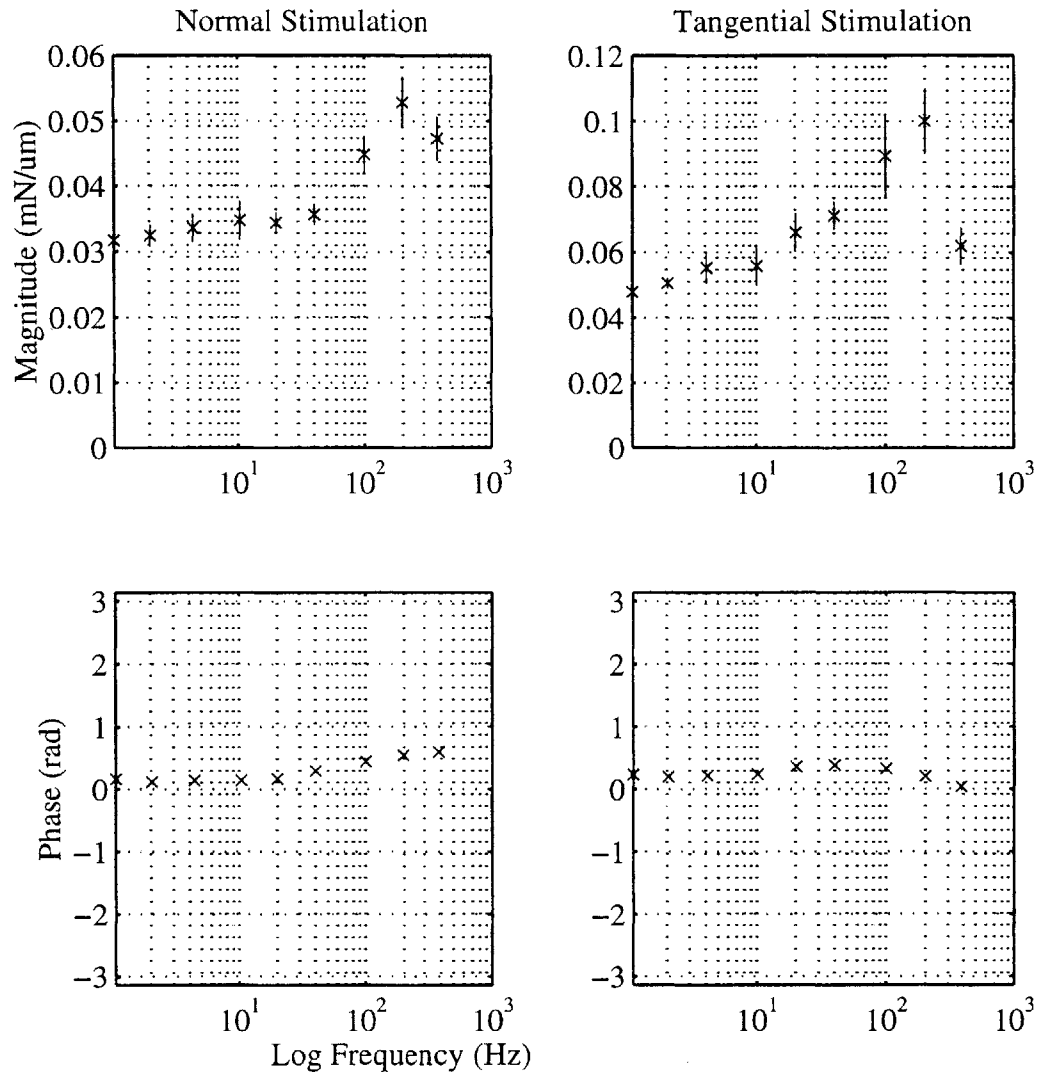
Fig. 4 (c) - Impedance magnitude and phase at the forearm for normal and tangential stimulation. The plots show the impedance averaged over five subjects at each body site. Error bars show standard deviation across subjects.
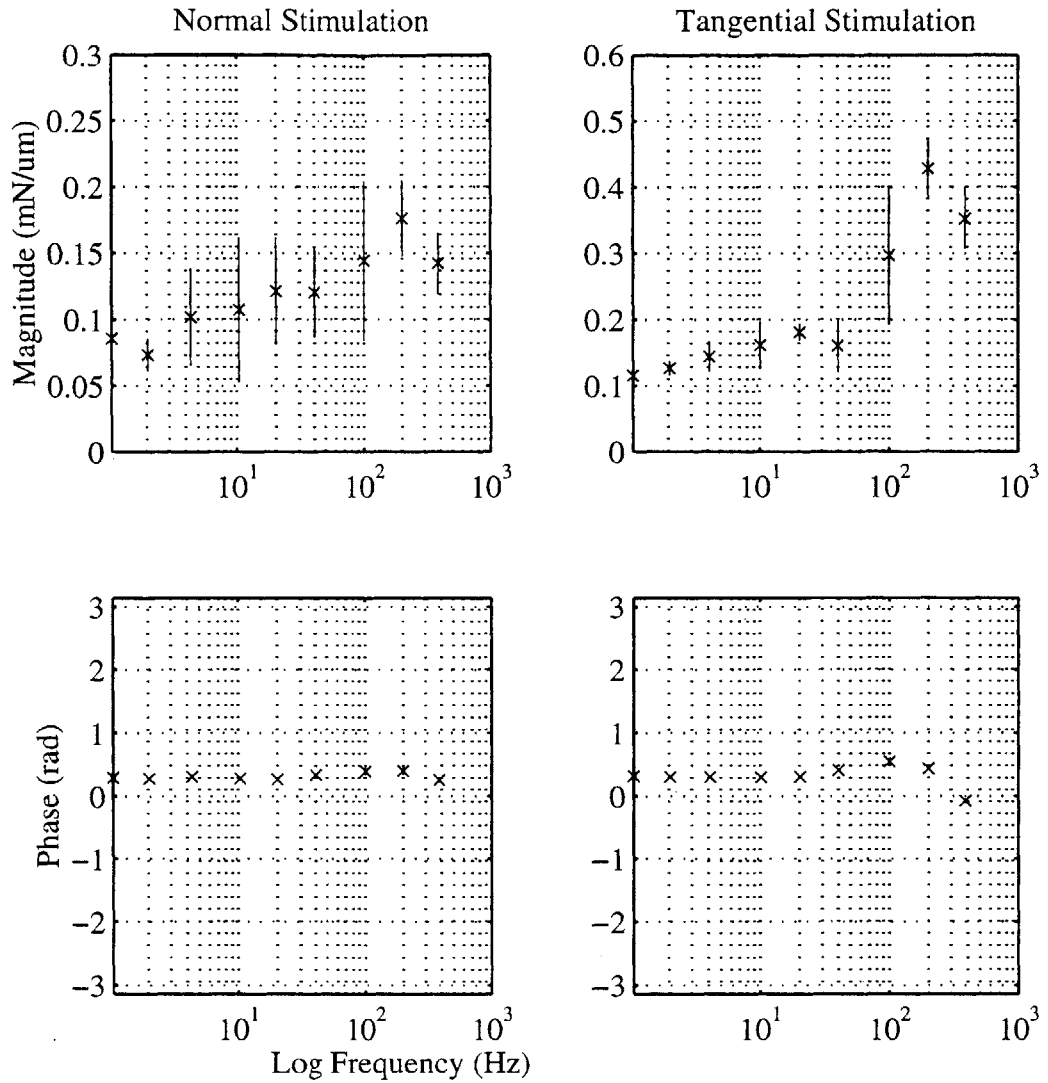
Fig. 4 (d) - Impedance magnitude and phase at the forehead for normal and tangential stimulation. The plots show the impedance averaged over five subjects at each body site. Error bars show standard deviation across subjects.

During measurements, noise from various sources such as subject motion, heartbeat, etc. tended to show up as variations in the force signal. Therefore, for calculation of mechanical impedance, the force data from the sinusoidal stimulation phase was filtered in MATLAB. The 'fir1' program was used to create a 256th order Hamming window filter with a pass band of ±10% of the stimulation frequency. This filter was then used in the

30

'filtfilt' program to filter the data for further processing. 'filtfilt' filters the data in both the forward and reverse directions to ensure zero phase distortion and does not introduce any transient effects at the ends of the data. This filtering produced a sinusoidal signal closely matching the original signal in amplitude and phase, yet without the noise.

The magnitude of the impedance S was calculated as the amplitude of the force signal $f(t)$ divided by the amplitude of the position signal $g(t)$. Numerically this was calculated as follows:

$$S = (\max_{cycle}(f(t)) - \min_{cycle}(f(t)))/(\max_{cycle}(g(t)) - \min_{cycle}(g(t))) \quad (3)$$

Phase lag ϕ in a single cycle was calculated by dividing the difference in the time values t_D and t_F where $g(t)$ and $f(t)$ crossed their mean values D_{mean} and F_{mean} with negative slope by the period T. D_{mean} and F_{mean} are averaged over the cycle under consideration.

$$t_D = g^{-1}(D_{mean}) \text{ for } dg/dt < 0 \quad (4)$$

$$t_F = f^{-1}(F_{mean}) \text{ for } df/dt < 0 \quad (5)$$

$$\phi = 2\pi(t_D - t_F)/T \quad (6)$$

Magnitude and phase were calculated for several cycles and averaged for each trial. The number of samples taken depended on the frequency of stimulation. Enough cycles were chosen to provide a good statistical sampling of the data without unnecessarily increasing the processing time. For example, in 1 Hz trials, starting with the second full wave, 4 waves were observed. In trials above 100 Hz, 150 waves were processed, starting with the second full wave.

Figure 5 compares the magnitude of the impedance vs. frequency among subjects at (a) the finger tip, (b) the wrist, (c) the forearm, and (d) the forehead. In these plots, the impedance magnitude is averaged over all stimulation amplitudes, and separate symbols were used for each subject. Lines connecting data points above 100 Hz are dashed to indicate that the data did not match our expectation that the magnitude of impedance would increase with

stimulation frequency. Although we thought that this might have been an artifact of the inertial compensation circuit in the probe controller, at the time of the writing of this thesis, this was not clearly understood, so the data are plotted as shown.
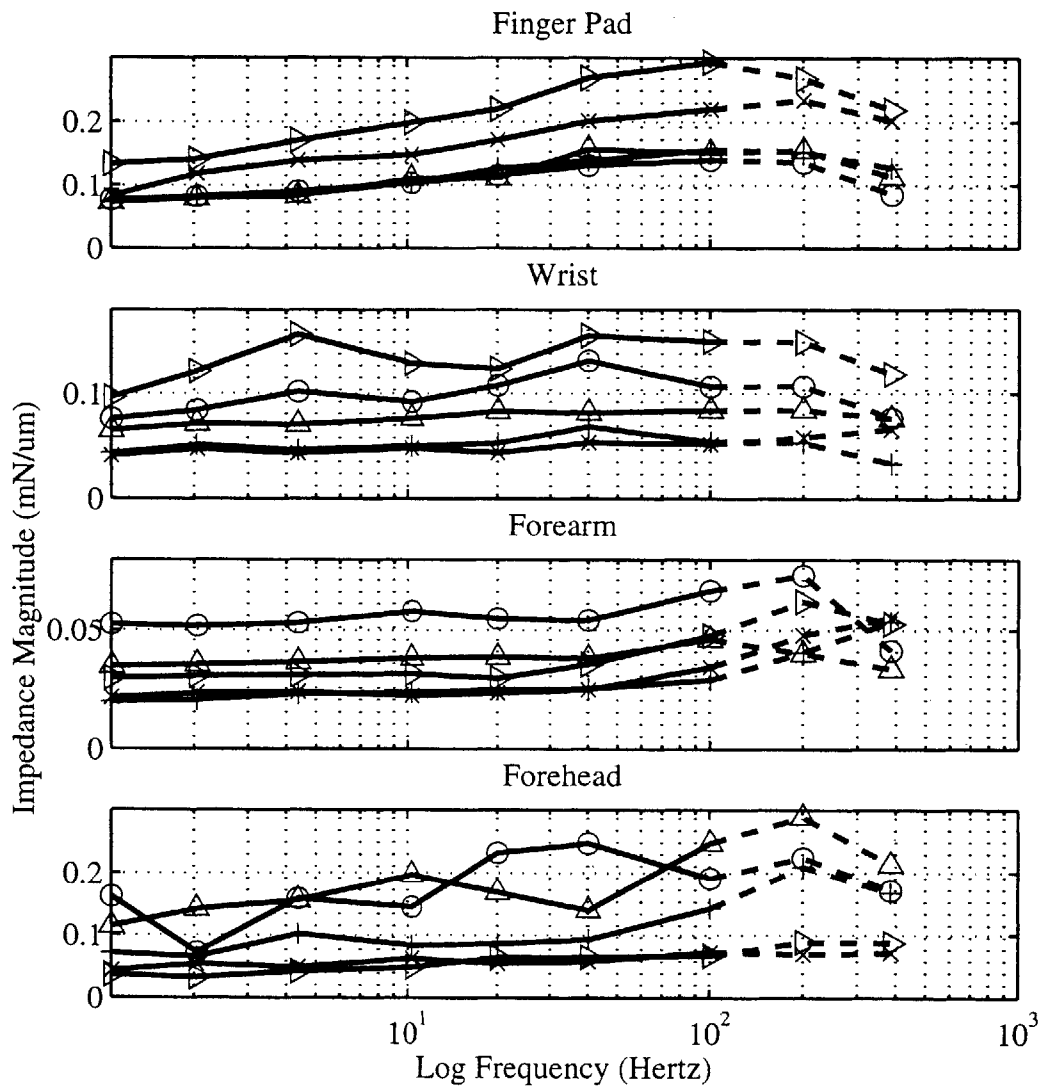

Fig. 5 - Comparison of impedance magnitude among five subjects at the finger pad, wrist, forearm, and forehead. Symbols differentiate between subjects in a plot, but do not represent the same subjects between plots. Magnitude of impedance is averaged across repetitions and amplitudes at each frequency.

Figure 6 shows the magnitude of the mechanical impedance averaged among subjects at every body site in (a) normal and (b) tangential stimulation. Data points in this

32

plot represent the average magnitude of impedance at each body site average over all the subjects. The same note from Figure 5 applies for Figure 6 concerning data above 100 Hz.
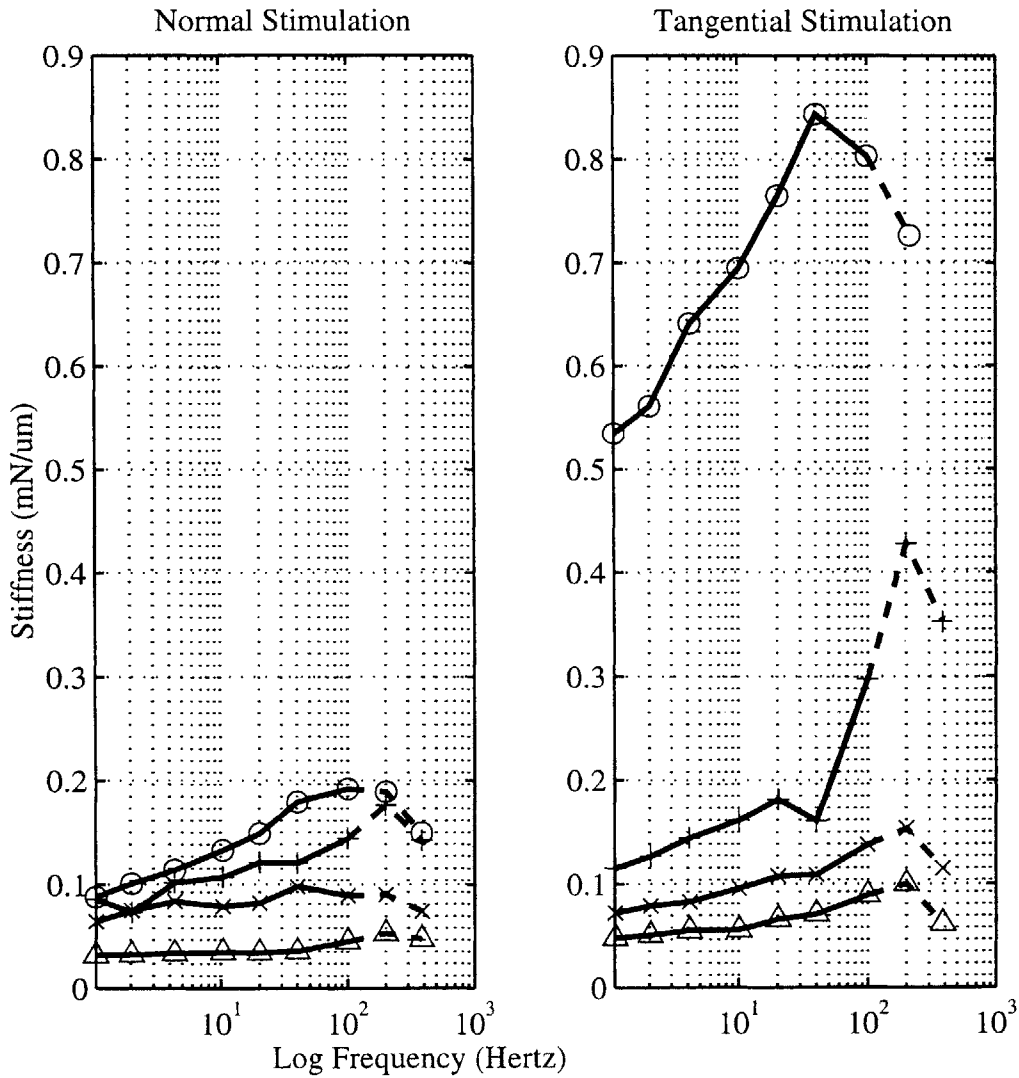
Fig. 6 - Comparison of impedance magnitudes between body site and stimulation direction. Data for each body site is an average of the five subjects tested there. Data points for the finger pad are marked with 'o', the wrist 'x', the forearm 'Δ', and the forehead '+'.

Because impedance is characterized by the ratio of output over input and phase angle, it is a transfer function for the material stimulated. Using equations (1) and (2), these mean transfer functions were used to calculate the equivalent bulk and shear moduli for an isotropic and semiinfinte material. However, at each body site, data from the subjects did not

meet the condition of the model that $2/3 < |T(s)| / |N(s)| < 4/3$. As a result, the bulk and shear moduli for these subjects had phases less than $-\pi/2$, or negative values of the modulus. At the wrist only, and for three subjects only, the equivalent bulk and shear moduli had a phase between $-\pi/2$ and $\pi/2$ from 1 to 100 Hz.

3.2. Non-Glued Tests

Figure 7 summarizes the results of the step indentation trials at each body site. Peak and steady-state forces are plotted against step depth. Peak force was measured as the maximum value of the force signal in the first 3 seconds of the trial. To find the steady state force, a moving average force over two seconds of data was taken. The interval was shifted one second and compared with the previous average. When the difference between the two was less than 10% of the peak force value, the current rolling average was taken as the steady state value. This method was chosen because variations in the force value were related to the depth of indentation and hence the peak force value at the end of the ramp. Data values shown here are averages across all repetitions and subjects per body site. Forces were averaged first over the repetitions for a single subject. Then these mean values were averaged across the subjects for the plots here. One sided error bars show the standard deviation of the averages across subjects. Due to a problem with the setup, step indentation trials were not run on subject #2, so for the finger pad, there is data for four subjects only. At the other body sites, data is averaged over five subjects. The linear fit lines were calculated with the MATLAB function "polyfit," which used the least squared error method.

34
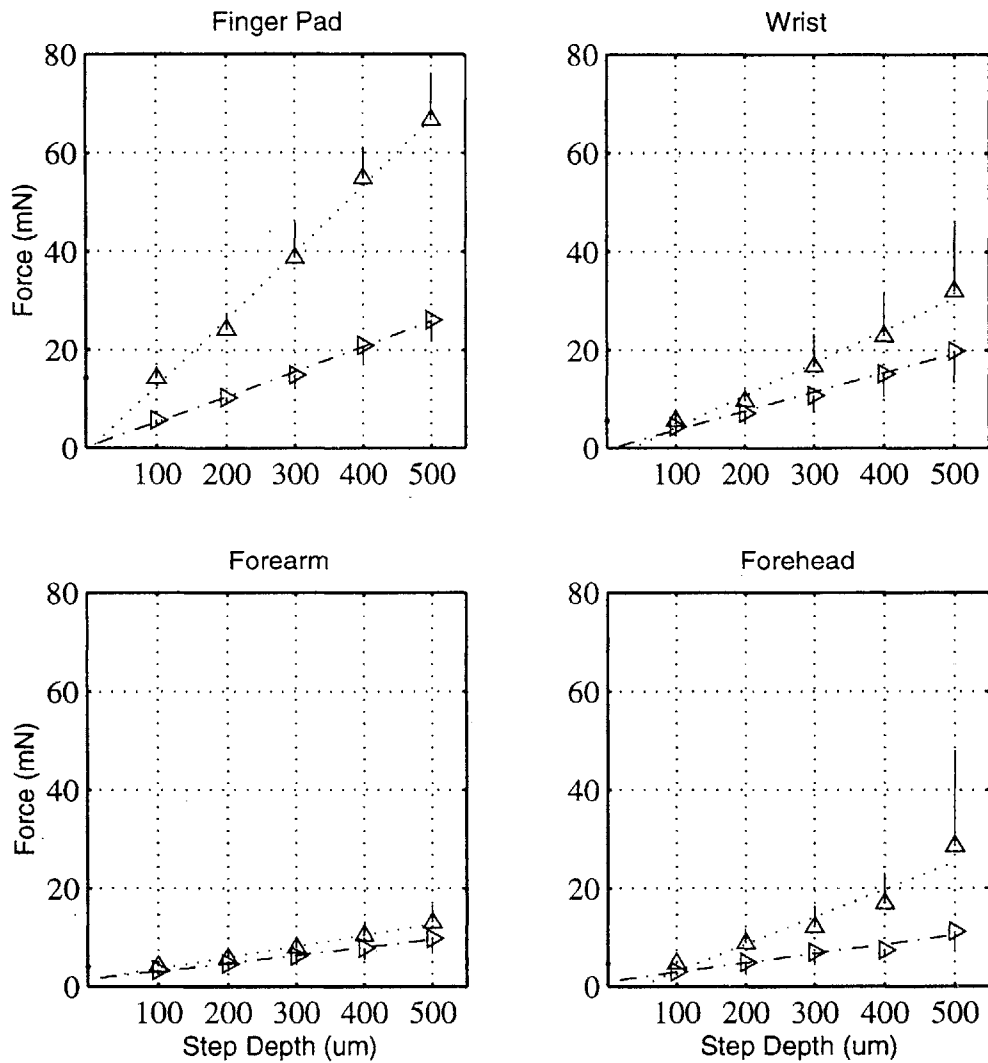
Fig. 7 - Step response data averaged across 4 subjects at the finger pad and 5 subjects at the other body sites. Peak force (upward pointing triangle) is the instantaneous force immediately after step displacement of the probe into the skin surface. Steady-state force (sideways pointing triangle) is the average force after viscoelastic relaxation has occurred. Error bars show standard deviation across subjects.

Figure 8 shows the average power absorption in the skin tissue as a function of frequency and amplitude at each of the body sites. Energy dissipation E during one stimulation cycle in the skin through hysteresis loss is equal to the path integral of the force with respect to the displacement around one full cycle:

$$E = \oint_{cycle} f\,dg \qquad\qquad (7)$$

Numerically, this is equivalent to the area inside one loop on the force-displacement plot and was calculated by summing the trapezoidal areas corresponding to two consecutive samples of the displacement. Recall that force and position measurements were offset in time by exactly half the sampling frequency. Therefore, in order to avoid introducing a phase shift of $\pi/40$ (4.5°), the force values were interpolated to match the exact time value of the corresponding position measurement.

$$E = \sum_{i=1}^{\#pts} \left((g_{i+1} - g_i)\left((f_{i-1} + f_i)/2 + (f_i + f_{i+1})/2 \right)/2 \right) \qquad\qquad (8)$$

Energy dissipation values of several cycles were averaged and plotted with respect to frequency. Average power was then calculated by multiplying this energy per cycle by the frequency. Because subject motion greatly increased the uncertainty of the actual mean depth of stimulation, the values plotted here are averaged over both of the nominal mean depths, 200 μm and 400 μm. This is further discussed in section 4.2 "Limitations." The results show that the power absorbed by the skin is approximately proportional to the frequency of stimulation. In the log-log plot shown in Figure 8, the initial vertical offset indicates the constant of proportionality as a function of stimulus amplitude.

36
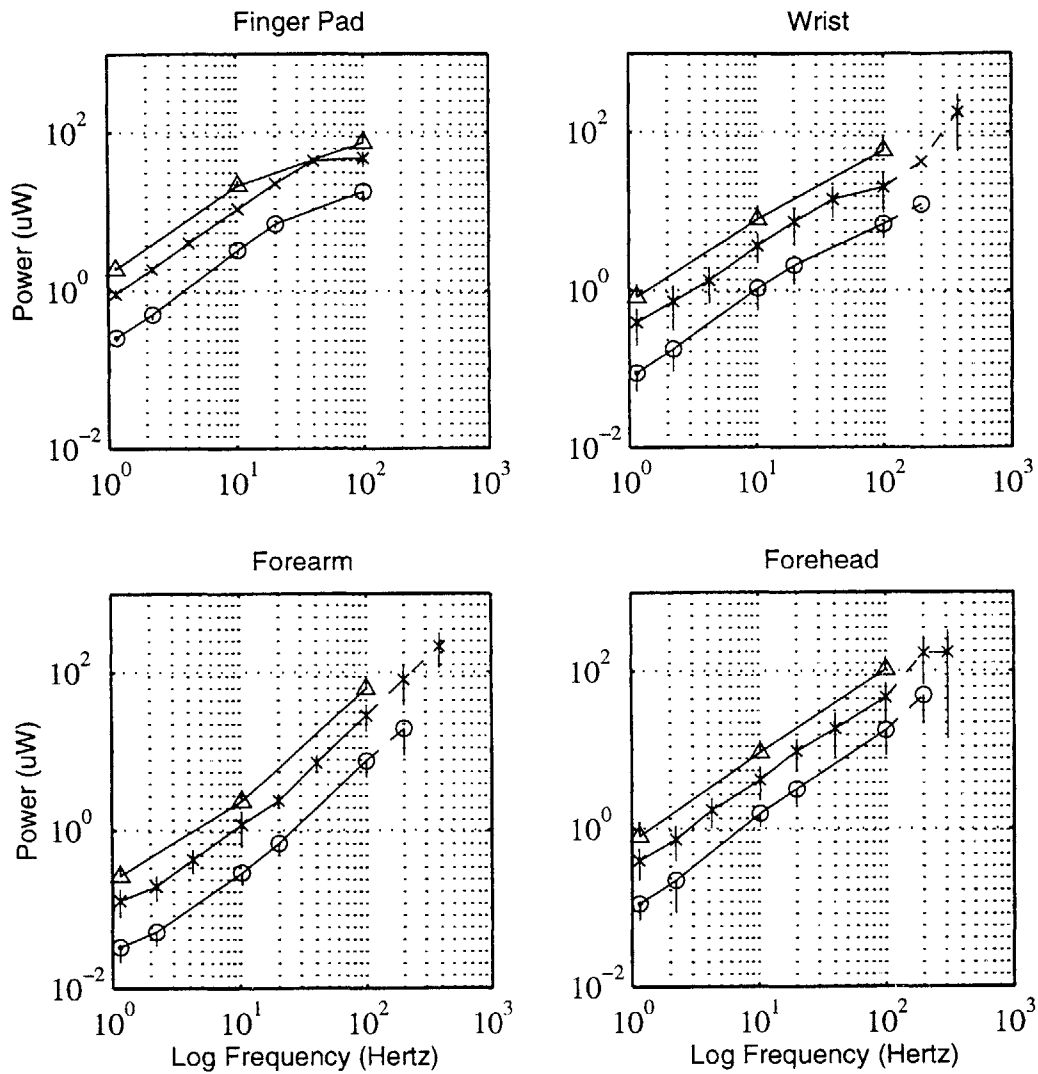
Fig. 8 - Average power dissipation through hysteresis averaged over all subjects at each body site. Power is calculated as the average area inside the force-displacement curve times the frequency of stimulation. Data points for three amplitudes of stimulation are shown at each body site: 50µm -'o', 100µm - 'x', and 150µm – 'Δ'. Error bars show standard deviation across subjects.

Duty factor is a measure of the continuity of contact between the probe and the skin surface. Figure 9 plots duty factor as a function of frequency at three amplitudes for the four body sites. A duty factor of 1 means the probe remained in contact with the skin for the entire cycle, and a duty factor of 0 means the probe never touched the skin. The points plotted are averages over five subjects, with error bars showing the standard deviation

among the subjects. As in Figure 8, the points are averaged over all mean depths of stimulation. For clarity, half bars are used for 50μm and 150μm amplitudes.
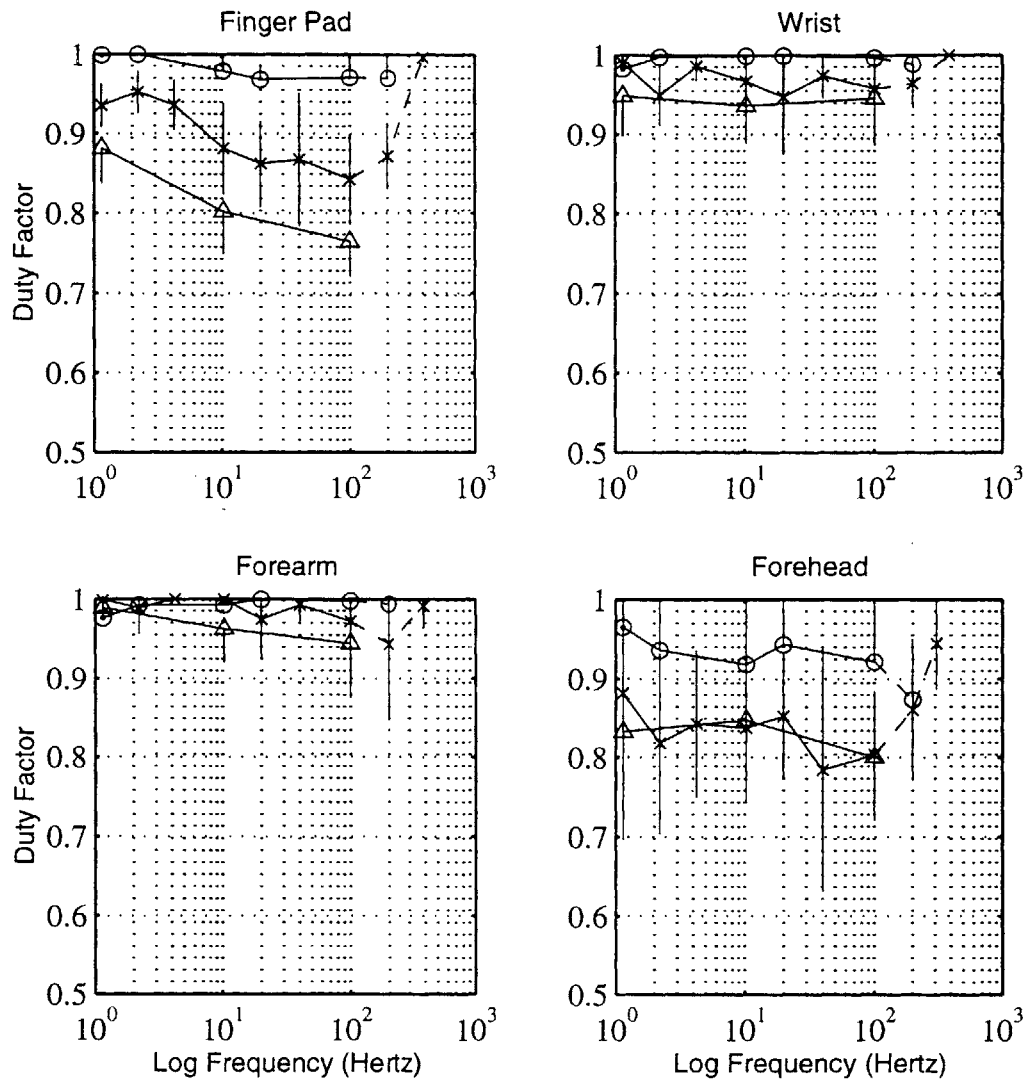
Fig. 9 - Duty factor for the probe, averaged across all subjects at each body site. Duty factor is an estimate of the ratio of the time the probe is in contact with the skin surface to the total time in a cycle. Data points for three amplitudes of stimulation are shown at each body site: 50μm - 'o', 100μm - 'x', and 150μm – 'Δ'. Error bars show standard deviation across subjects.

Duty factor was calculated as an average ratio of the number of data points for which the probe was in contact with the skin surface to the total number of data points in one stimulation cycle. Care was taken to measure the points whose force actually resembled those in contact with the skin surface. In some instances, it was observed that in non-glued

38

trials, the force became slightly negative before becoming zero. Merely counting the number of positive force points would not have accounted for this. In addition, if a force was measured at zero, yet its slope was positive, then this indicated that the probe was still in contact with the skin surface.

Therefore, in one stimulation cycle, if a force measurement was outside a small dead-band around zero equal to the uncertainty in the force signal (±0.5 mN), it was considered to be in contact with the skin surface. If the point was inside the dead-band and its slope was greater than or equal to 0.03 mN/μm, then it was considered to be in contact with the skin surface, 0.03 mN/μm was the smallest force-displacement slope seen in glued trials. The curve in Figure 3(b), for example, has a duty factor of 0.79.

3.3. Analysis of Uncertainty

Uncertainty in the measurements came from four primary sources: electrical noise in the transducers, the resolution of the data acquisition hardware, the limited ability of the controller to compensate for the inertia of probe, and the motion of subjects during testing. Uncertainty of the timer was ignored due to its small magnitude [National Instruments 1992].

Using the root-sum-squares method [Figliola & Beasley 1995], the combined uncertainty from electrical noise and data acquisition resolution in the force and position measurements were 0.51mN and 1.9μm, respectively. Uncertainty in the calculated phase, based on a typical signal of 50μm positional amplitude and 5mN force amplitude, was 0.17 radians, or an error of about 2.7% over 2π radians. Uncertainty in the calculated magnitude of the impedance was 0.077 mN/μm based on signals of the same magnitude. Uncertainty in the energy per cycle was ±11 nJ. Consequently uncertainty in the power varied with frequency from ±11 nW at 1Hz to ±4.4μW at 400 Hz.

Although every effort was made to minimize the amount of glue used and to achieve consistency, the amount did vary, and measurement of the actual amount of glue used was quite difficult. In addition, estimation of the size of the meniscus was complicated by the non-uniformity of the skin surface. That is, capillary action may have drawn the glue into the papillary ridges, depending on the positioning of the probe. This made it quite difficult to define the boundaries of the meniscus. In addition, because the mechanical properties of the glue differed significantly from both the skin and the probe, estimation of the effective diameter of the probe tip is further complicated. Its minimum value can be safely set at 0.50 mm, the diameter of the probe tip. From inspection of the meniscus after removal of the probe from the skin, it is known that the maximum extent of the thinnest part of the meniscus in some cases reached 1 mm. If we estimate that due to the thinning of glue with the radius of the meniscus, the effective diameter of the meniscus is about a third the actual diameter added to the minimum diameter, then the effective diameter of the probe would have varied between 0.50 and 0.70 mm, a ±20% uncertainty.

Although the body site being measured was immobilized as much as possible, motion of the subject relative to the probe was inevitable due to periodic variations in blood pressure, breathing, nervous twitches and various other causes. In the finger pad, pulse from the heartbeat was most clearly evident in the step indentation trials and depended on the indentation depth: at 100μm indentation, a 1Hz, 2mN peak-to-peak pulse is evident. At 500μm indentation, the pulse appears with an amplitude of 10mN, peak-to-peak. In the wrist and forearm, subject motion was much less regular and was not strongly dependent on indentation depth. A variation coincident with the subject's breathing is apparent in some trials, with a period of roughly 5 seconds and a peak-to-peak amplitude of 2-5mN. Effectively immobilizing a subject for measurements on the forehead proved to be the most problematic. The discomfort associated with immobilization of the head and neck varied considerably among the subjects tested as did, consequently, the error introduced through

40

subject motion. In some trials, abnormal subject motion caused an error with a magnitude great enough (>>10mN) to warrant removal of that trial from the analysis.

The probe was run in air at the same frequencies and amplitudes used in the measurements. From 1 – 100 Hz, the force signal was ±0.5 mN, which is within the noise resolution of the sensors. At 200 Hz, a force signal with a peak-to-peak amplitude of 2 mN was seen when the probe was vibrated at 300μm peak-to-peak amplitude. At 400 Hz, with the same vibration amplitude, the force signal had a peak-to-peak amplitude of 6 mN.

Variation among the subjects was considerably higher than the noise levels from the instrumentation. At the finger pad, for instance, under normal stimulation, stiffness of the stiffest subjects was consistently more than twice as stiff as that of the least stiff subject over the entire frequency range.

Chapter 4: Discussion

4.1. Trends

Impedance magnitude was most strongly dependent on frequency at the finger pad, although in general, it increased with frequency at every body site. 200 Hz and 400 Hz measurements were exceptions, however, and we believe this to be an artifact of the inertia compensator, as discussed in the uncertainty analysis section of chapter 3. It is not completely clear how the inertia compensation is implemented in the Aurora controller, because merely subtracting the signal generated in air from the signal generated in contact with the skin surface does not produce an impedance magnitude monotonically increasing with frequency. Rather than being a simple additive signal that can be subtracted when the amplitudes of stimulation are the same, we believe that the 'no-load' signal may change with loading since the input signal must be changed to account for attenuation of amplitude at the higher frequencies. Further investigation is necessary before any conclusions can be drawn about the behavior of the skin at frequencies of 200 Hz and higher.

The impedance phase was generally around 0.2 radians and not dependent on frequency, suggesting that at the scale tested and at these body sites, human skin behaves primarily like a spring with a small damping component and without inertial effects. When we tested the post-processing data analysis system with artificial data, force-displacement data from a pure spring model yielded impedances which did not depend on frequency and whose phase shift was zero. A pure damping model yielded force-displacement data with impedance magnitude proportional to frequency and with phase shift of $\pi/2$. The measured

data show a linear dependence on frequency and a small phase shift, which is consistent with our understanding of human skin tissue as a viscoelastic material.

In addition, the tissues fulfilled three criteria proposed by De and Srinivasan [2001] for characterization as viscoelastic materials. In Fig. 7, we see that the steady state value of the force on the probe is a linear function of the depth of indentation. In Figure 2, stress relaxation after the preindentation is exponential in nature, and the force displacement loop in Fig. 3 shows the dissipation of energy through hysteresis.

The assumptions of the model, however, proved to be inappropriate. The model assumed that the skin and underlying tissue were isotropic, semi-infinite, and loaded under static conditions. According to Equations (1) and (2), in order to provide positive, real, finite values for the bulk and shear moduli, the magnitude of the tangential stimulation transfer function should have fallen in the range $2/3N(s) < T(s) < 4/3N(s)$. However, at the finger pad, the magnitude of impedance in tangential stimulation was consistently five times greater than the magnitude of impedance in normal stimulation. At the other body sites, impedance in tangential stimulation was higher than four-thirds the impedance in normal stimulation. Causes for higher tangential impedance include anisotropy and finite thickness of the skin and underlying tissues. Another limitation of the model came from the assumption that the stimulation was quasi-static, limiting the validity of the bulk and shear modulus calculations to 200Hz and less [De 2000]. The effect of violating these assumptions was that the moduli had phases which at some frequencies were below $-\pi/2$ or above $\pi/2$, making the modulus negative in value.

4.2. Limitations

The study was limited by several factors. First was the limited ability of the hardware to measure forces effectively at frequencies higher than 100 Hz. Measurements at higher frequencies could be of considerable value in dynamic modeling, but the ability of

44

the controller to compensate for the inertia of the probe arm and tip began to degrade at 200 Hz. This brought greater uncertainty to other measurements as well.

For instance, the duty factor of the indentor (Fig. 9) in some cases shows a minimum between 100 Hz and 200 Hz. We did not expect to see a higher duty factor at 400 Hz than 200 Hz. This can be attributed in large part to the degradation of the inertial compensation system, because the error in the signal at 200 Hz and 400 Hz exceeds the uncertainty for lower frequencies. Therefore, points for which the probe was actually off the skin have a force measurement which lies outside the dead band, and consequently appear to the duty factor analysis algorithm to be in contact with the skin.

The size of the subject population was small, and because not all body sites were measured for each subject, evaluation of differences among body sites is of limited value. In addition, subjects varied widely in both the mechanical properties of their skin and in their overall response to the tests. That is, the ability to remain still and be comfortable for the required time period varied among the subjects. Consequently, the amount of movement apparent in the force data depended quite strongly on both the subject and the body site. A big challenge for future research will be to develop methods for effectively immobilizing the body site under study. This includes ensuring the comfort of the subjects, which in our measurements, was a strongly determined of how little noise was in the data due to subject motion.

Several problem resulted from the size of the probe used, primarily related to gluing the probe to the skin. Use of a probe with a larger diameter could have reduced some of the problems associated with the use of glue, so the size of the glue meniscus relative to the indentor would have been smaller. Also, because the diameter of the probe was of the same magnitude as the size of papillary ridges on the finger pad, placement of the probe with respect to the ridges may affect the measurement. No effort was made to consistently position the probe with respect to the ridges in finger pad measurements, so the effect of stimulating of the ridges versus the vallies is not known in this study.

In the end, the mean depth of stimulation was removed from consideration as a variable, not because it did not affect the measurements, but rather due to the difficulty of controlling and determining its actual value, in particular at the forehead. If a subject moved relative to the probe during the course of a trial, this would not reflect in the position signal, which assumed that the skin surface was stationary with respect to the probe position. Rather, it would appear as a change in the value of the force, where it might be difficult to distinguish from the signal itself or from a variation in surface pressure due to blood flow, for instance. However, because stimulation was restricted to a linear range in the skin, impedance was not a function of the mean depth, and power absorption and duty factor were averaged across mean depths. The effect of depth of stimulation on force was well captured by the step indentation trials summarized in Fig. 7, which were closely screened for subject motion in post-processing.

4.3. Implications for Design of Tactile Displays

Variation in the impedance among subjects was high, which has significant implications for tactile display design. That is, a tactile display must be capable of operating over a wide variety of conditions. Note that the subject population in this study was homogenous with regard to the use of hands: none of the subjects did significant manual labor. In a real world application, no such restrictions will apply, and a display device will have to operate effectively on skin which is significantly tougher, more callused, less clean, and at a wider range of temperatures than was tested in this study. Variations in moisture content of the skin, which in this study was controlled by hand washing, the absence of sweat, and sedentary condition of the subjects, will also impact the properties of the skin.

A designer of a tactile display should also be aware that contact between the stimulator and the skin surface is not constant and tends to decrease with increasing amplitude and frequency. Yet, it is interesting to note that in Fig. 8, power is linear with respect to frequency in a log-log plot. This indicates that the energy dissipation is only

46

weakly dependent on stimulation frequency. Comparison of power absorption data with duty factor data in Fig. 9 seems to indicate that power absorption is not strongly tied to duty factor. Preliminary research conducted in our laboratory that is not yet published suggests that while the amplitude threshold of human perception drops with frequency, the power threshold does not. If this is confirmed in further study, it suggests that perhaps tactile displays should be designed to deliver stimulation by metering power absorption rather than stimulation amplitude.

Finally, human tactile perception is itself frequency dependent. At around 256 Hz, human threshold detection is at its peak when the Pacinian Corpuscles (PC's) are excited. However, the spatial distribution of PC's is very low, and human spatial resolution is higher at lower frequencies. While not directly related to this project, this suggests that from a performance perspective, attenuation of stimulation amplitude with increasing frequency in a tactile display might not be a major problem.

4.4. Conclusions

We have characterized the frequency-dependent interaction of human skin with a small radius indentor in terms of the force-displacement relationship under dynamic loading in two directions, the static loading characteristics, the power absorption by the skin, and the constancy of contact between the indentor and skin surface. We have provided previously unavailable specifications for the development of tactile displays. By simulating the interaction of a single MEMS stimulator with the skin surface we have shown the range and nature of forces to be encountered in a tactile display.

In addition, a mathematical model of the stimulation was tested against empirical data, and several of the key assumptions of that model were found to be invalid, notably, the isotropic assumption. This result seems to suggest that internal structure plays a significant role in the mechanics of the skin and underlying tissue.

Future work should focus on refining these measurements, particularly with regard to increasing the high-frequency resolution of the sensors and minimizing the motion and discomfort of subjects during testing (especially at the forehead.) Complementary studies focusing on the psychophysical response of human subjects to the same stimuli used here will provide much more insight and guidance in the design of tactile displays.

Furthermore, it would be interesting to explore the effects of the direction of stimulation with respect to the papillary ridges of the finger pad on both the material properties of and psychophysical response at the finger pad.

BIBLIOGRAPHY

Birch, A. S., 1999 "Experimental Determination of the Viscoelastic Properties of the Human Fingerpad," *Touch Lab Report 14, RLE TR-632*, Massachusetts Institute of Technology, Cambridge, MA

De. S, 2000, *Unpublished observations*, The Touch Lab, MIT, Cambridge, MA

De. S., and Srinivasan, M. A., 2001, "A Finite Element Model of the Human Fingerpad Incorporating Viscoelasticity," *manuscript in preparation*

Figliola, R. S., and Beasley, D. E., 1995, Theory and Design for Mechanical Measurements, John Wiley & Sons, Inc., New York, pp. 171-209

Franke, E. K., 1951, "Mechanical Impedance Measurements of the Human Body Surface," USAF WADC, Dayton, OH, Technical Report 6469

Gulati, R. J., Srinivasan, M. A., 1995, "Human Fingerpad Under Indentation I: Static and Dynamic Force Response," *Bioengineering Conference*, **BED-29**, pp. 261-262

Hajian, A. Z., and Howe, R. D., 1997, "Identification of the Mechanical Impedance at the Human Finger Tip," *Journal of Biomechanical Engineering*, **119**, pp. 109-114

Johnson, K. L., 1985, Contact Mechanics, Cambridge University Press, Cambridge

Karason, S. and Srinivasan, M. A., 1995, "Passive Human Grasp Control of an Active Instrumented Object," *Proceedings of the ASME Dynamic Systems and Control Division,* **57-2**, pp. 641-647

Lee, E. H., 1955, "Stress Analysis in Viscoelastic Bodies," *Quarterly Applied Mathematics,* **13**, pp. 183-190

Moore, T. J., 1970, "A Survey of the Mechanical Characteristics of Skin and Tissue in Response to Vibratory Stimulation," *IEEE Transactions of Man-Machine Systems,* **MMS-11**, pp.79-84

Moore, T. J., and Mundie, J. R., 1972, "Measurement of the Specific Mechanical Impedance of the Skin: Effects of Static Force, Site of Stimulation, Area of Probe, and Presence of a Surround," *The Journal of the Acoustical Society of America,* **52**, pp. 577-584

National Instruments, 1992, *AT-MIO-64F-5 User Manual,* Austin, TX

Oestreicher, H. L., 1950, "A Theory of the Propagation of Mechanical Vibrations in Human and Animal Tissue," USAF WADC, Dayton, OH, Technical Report 6244

Pawluk, D. V. T., and Howe, R. D., 1996, "Dynamic Contact Mechanics of the Human Fingerpad, Part II: Distributed Response," *Harvard Robotics Lab Technical Report 96-004,* Harvard University, Cambridge, MA

Pawluk, D. T. V., and Howe, R. D., 1999, "Dynamic Contact of the Human Fingerpad Against a Flat Surface," *Journal of Biomechanical Engineering,* **121**, pp. 605-611

50

Serina, E. R., Mote, C. D. Jr., Rempel, D., 1997, "Force Response of the Fingertip Pulp to Repeated Compression – Effects of Loading Rate, Loading Angle, and Anthropometry," *Journal of Biomechanics*, **10**, pp.1035-1040

Srinivasan, M. A., 1989, "Surface Deflection of Primate Fingertip Under Line Load," *Journal of Biomechanics*, **4**, pp.343-349

Srinivasan, M. A., and Basdogan, C., 1997, "Haptics in Virtual Environments: Taxonomy, Research Status, and Challenges," *Computers and Graphics*, **21**, pp. 393-404

Srinivasan, M. A., Basdogan, C., and Ho, C. H., 1999, "Haptic Interactions in Virtual Worlds: Progress and Prospects," *Proceedings of the International Conference on Smart Materials, Structures, and Systems*, Indian Institute of Science, Bangalore, India.

Srinivasan, M. A., Dandekar, K., 1992, "Role of Fingertip Geometry in the Transmission of Tactile Mechanical Signals," *Advances in Bioengineering*, **BED-22**, 569-572

Srinivasan, M. A., Gulati, R. J., Dandekar, K., 1992, "In Vivo Compressibility of the Human Fingertip," *Advances in Bioengineering*, **BED-22**, pp. 573-576

Srinivasan, M. A., Gulati, R. J., and De, S., 2001, "Force Response of the Human Fingerpad to Dynamic Indentations," *manuscript in preparation*

Tschoegl, N. W., 1989, The Phenomenological Theory of Linear Viscoelastic Behavior, Springer-Verlag, Berlin, pp. 37-51, 136-145, 508-515
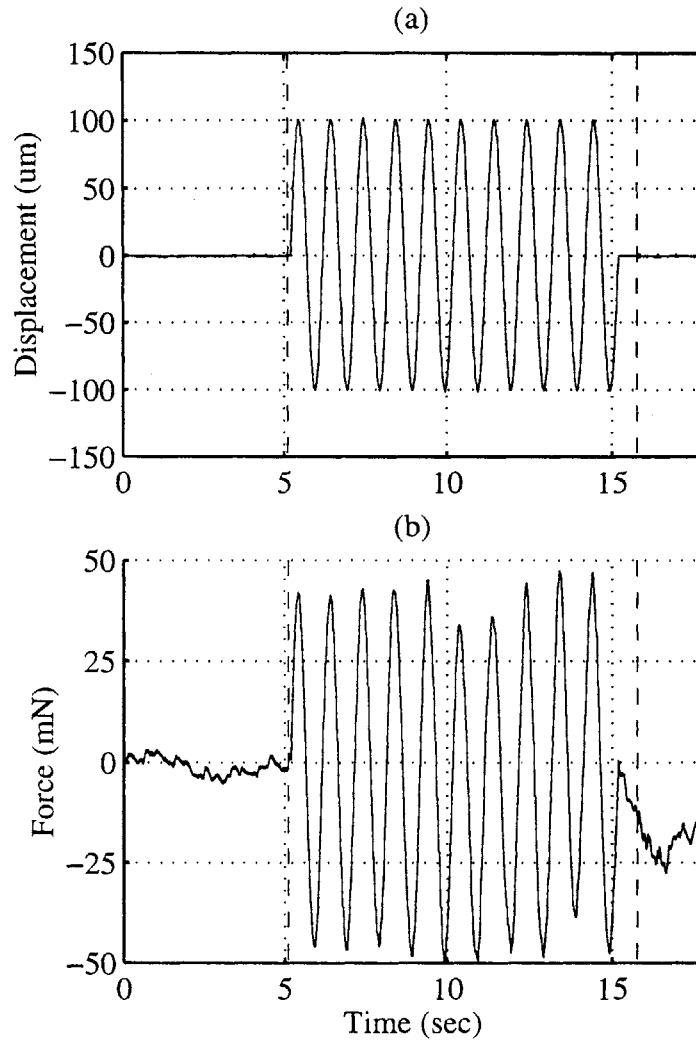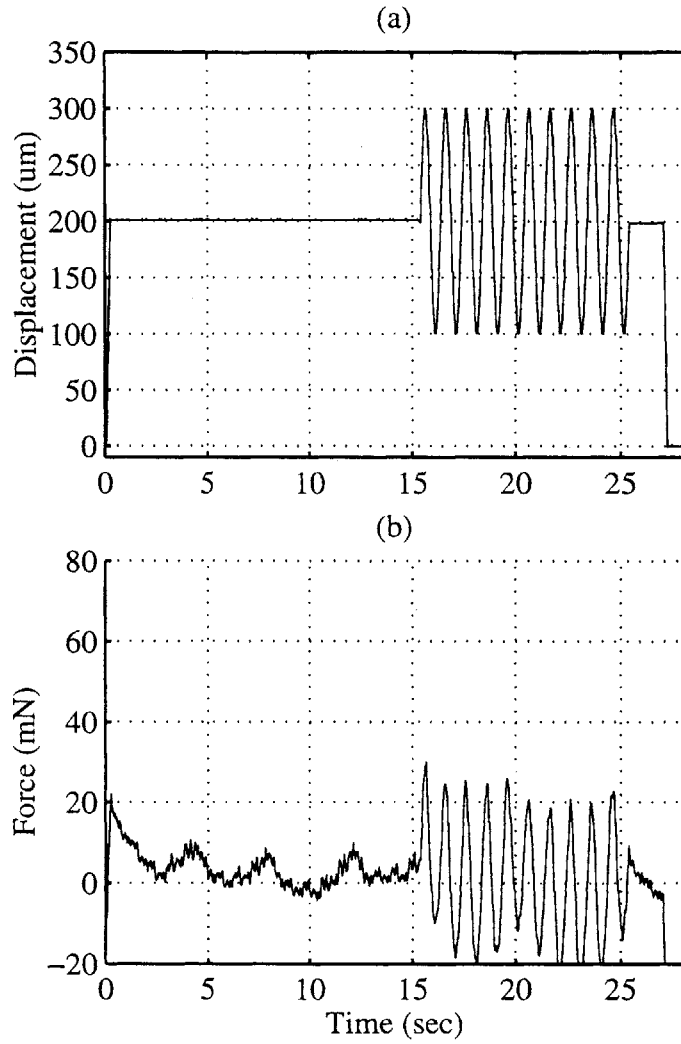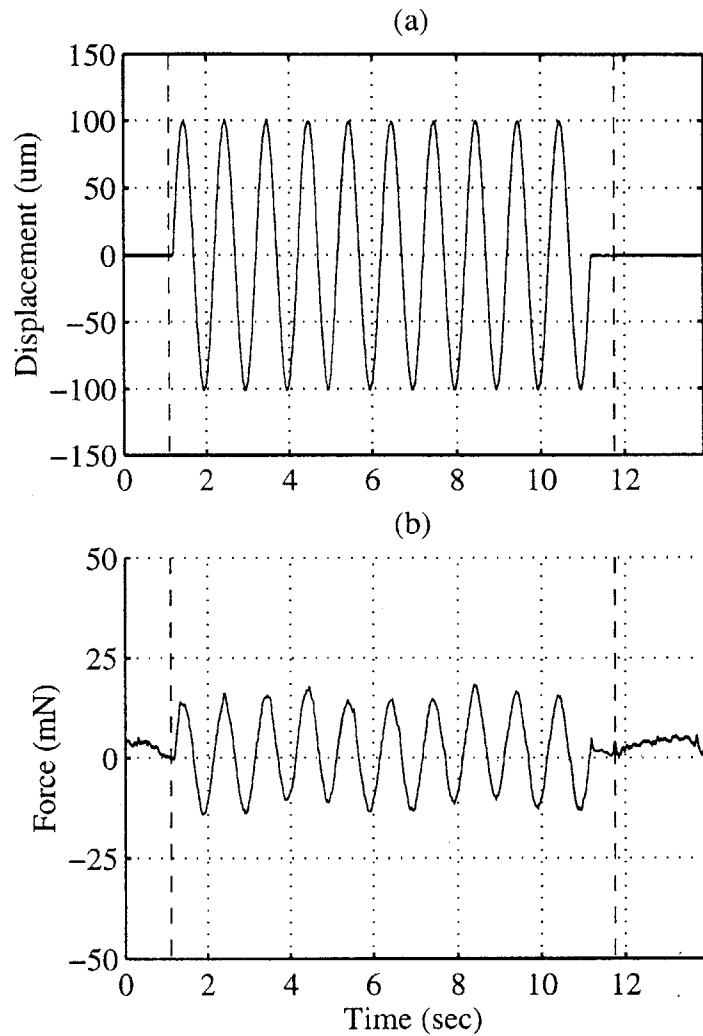
Figure A2.1: Stimulus and response of subject #3 at the finger pad with the probe glued; Stimulation is in the tangential direction at 1 Hz with 100μm amplitude. Preindentation is 200μm; (a) is the displacement input, and (b) is the force response.
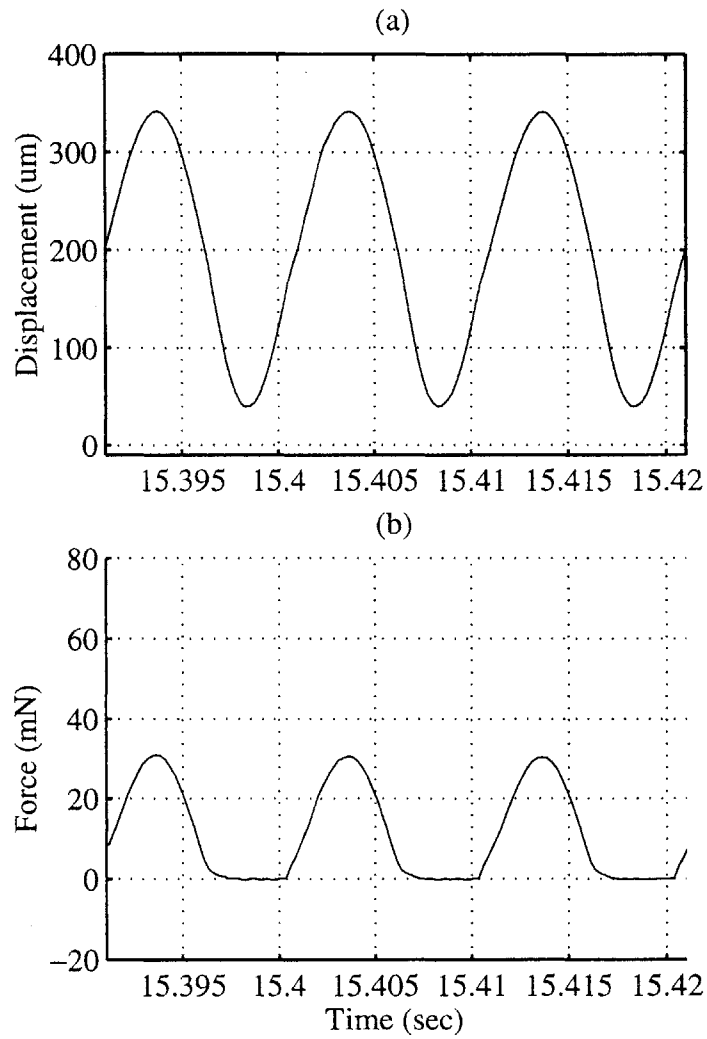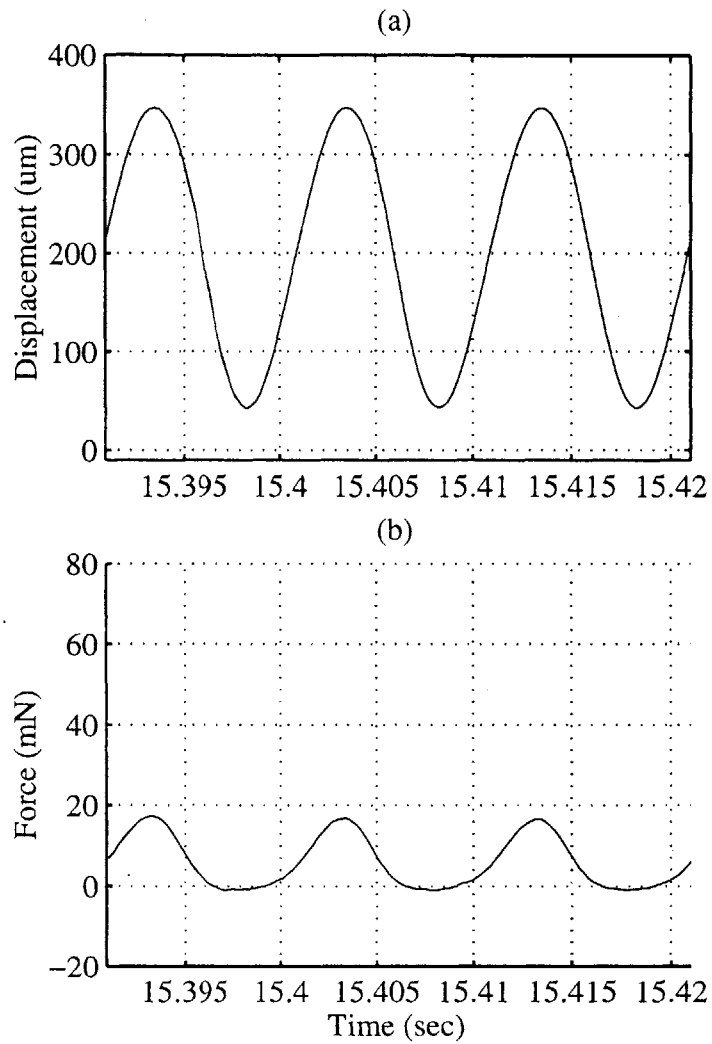
Figure A2.2: Stimulus and response of subject #3 at the finger pad with the probe not glued; Stimulation is in the normal direction at 100 Hz with 150μm amplitude. Preindentation is 200μm; (a) is the displacement input, and (b) is the force response. For clarity, only three cycles in the sinusoidal stimulation are shown.
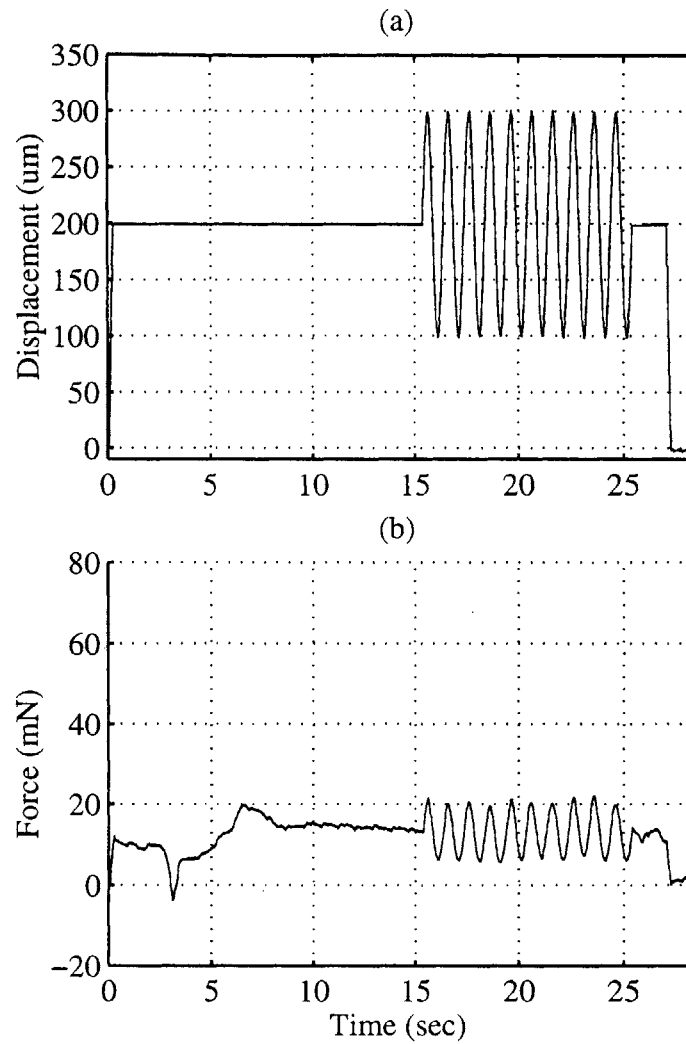
Figure A2.3: Stimulus and response of subject #3 at the wrist with the probe glued; Stimulation is in the tangential direction at 1 Hz with 100μm amplitude. Preindentation is 200μm; (a) is the displacement input, and (b) is the force response.
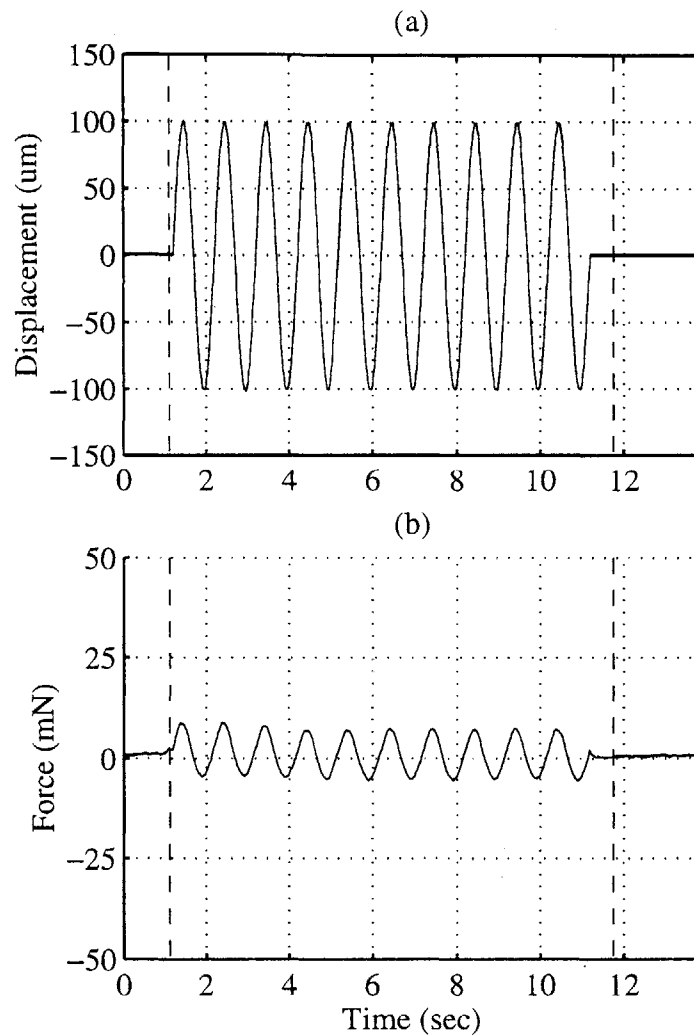
Figure A2.4: Stimulus and response of subject #3 at the wrist with the probe glued; Stimulation is in the tangential direction at 1 Hz with 100μm amplitude. Preindentation is 200μm; (a) is the displacement input, and (b) is the force response.
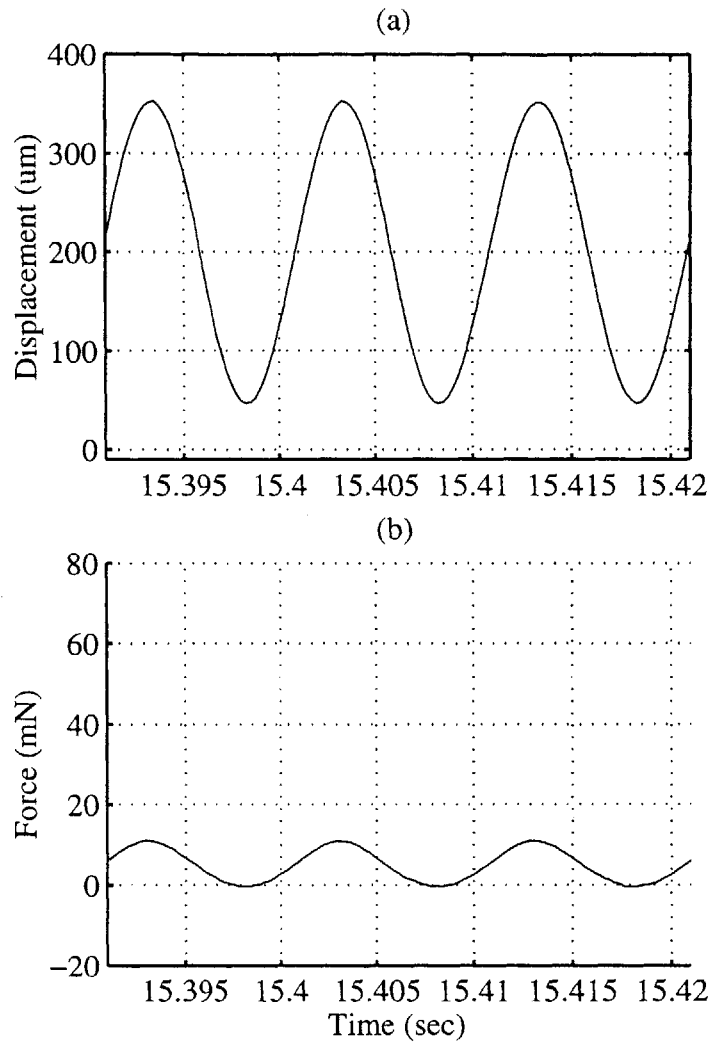
Figure A2.5: Stimulus and response of subject #3 at the wrist with the probe not glued; Stimulation is in the normal direction at 100 Hz with 150μm amplitude. Preindentation is 200μm; (a) is the displacement input, and (b) is the force response. For clarity, only three cycles in the sinusoidal stimulation are shown.
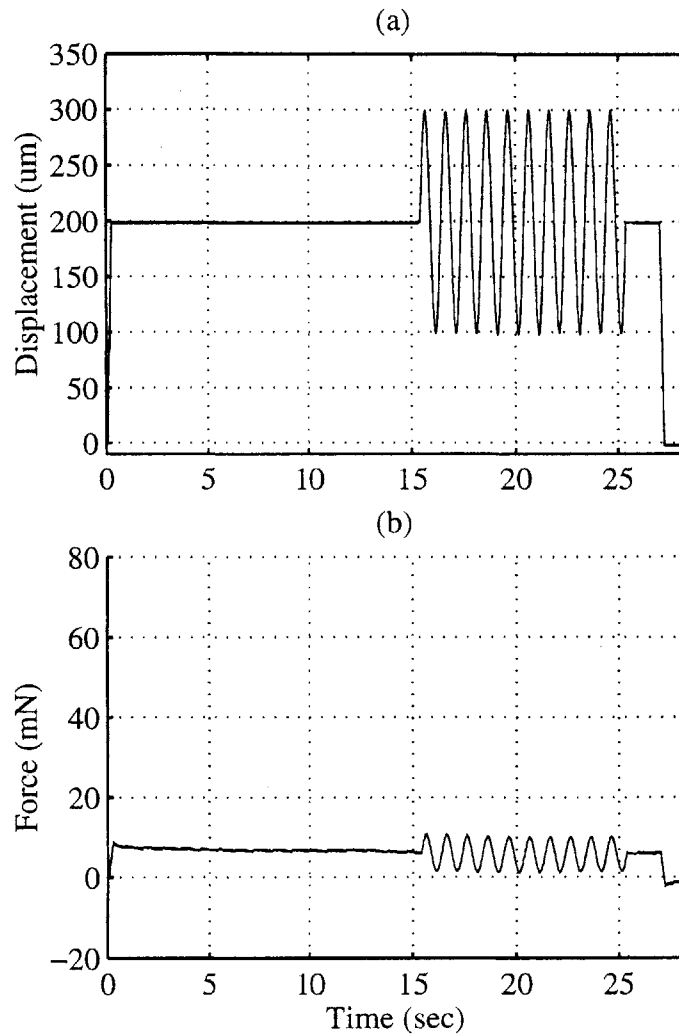
Figure A2.6: Stimulus and response of subject #3 at the forearm with the probe glued; Stimulation is in the tangential direction at 1 Hz with 100μm amplitude. Preindentation is 200μm; (a) is the displacement input, and (b) is the force response.
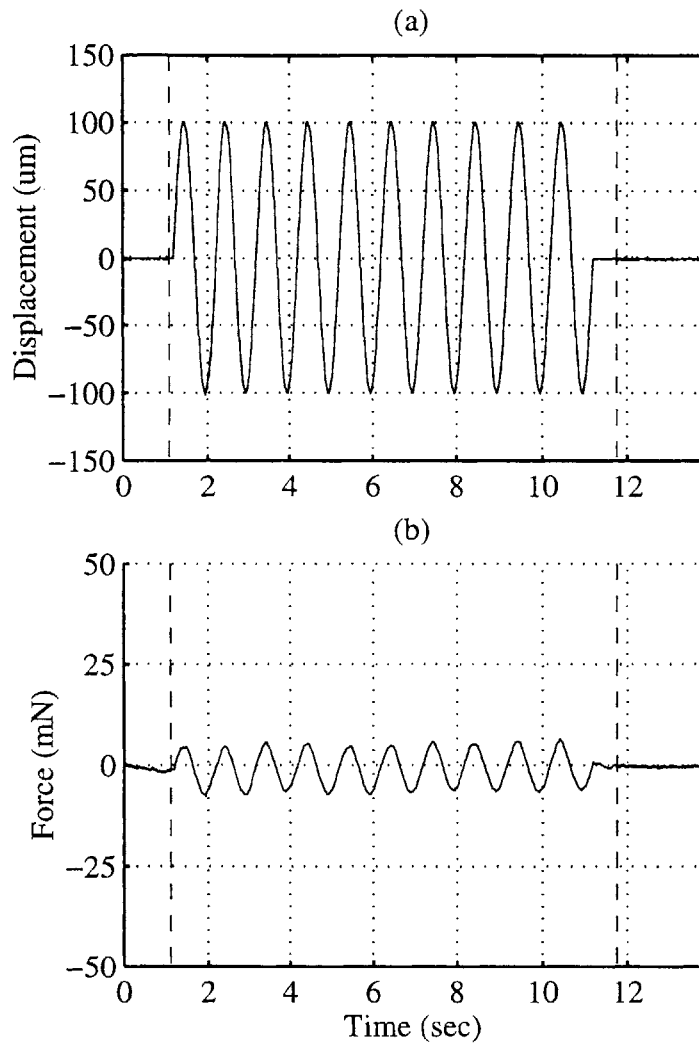
Figure A2.7: Stimulus and response of subject #3 at the forearm with the probe glued; Stimulation is in the tangential direction at 1 Hz with 100μm amplitude. Preindentation is 200μm; (a) is the displacement input, and (b) is the force response.
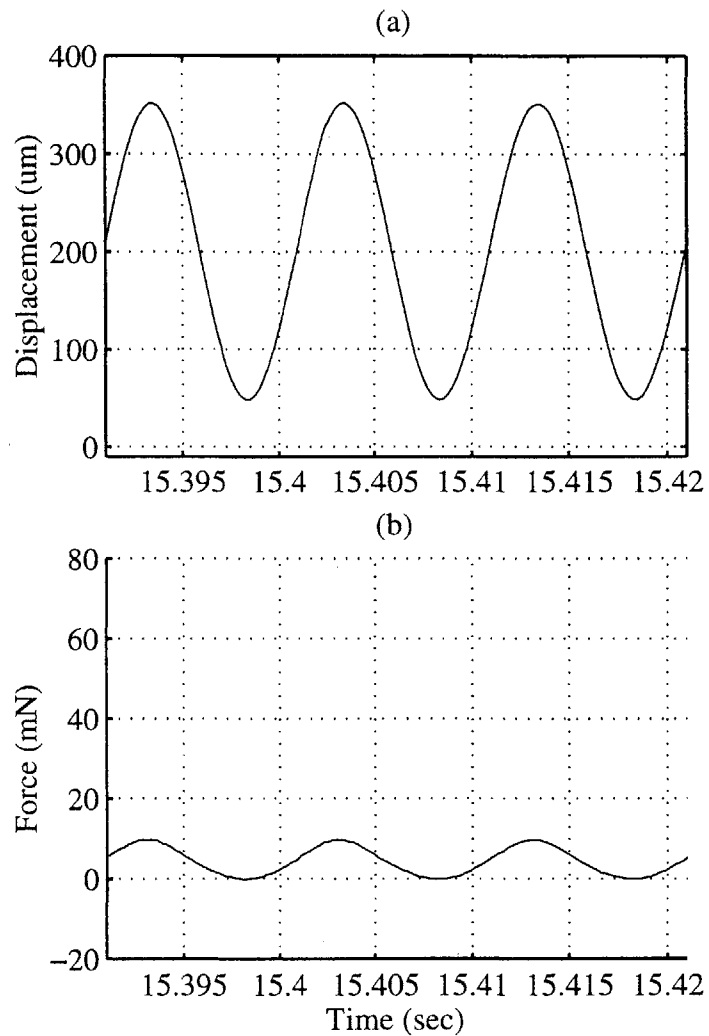
Figure A2.8: Stimulus and response of subject #3 at the forearm with the probe not glued; Stimulation is in the normal direction at 100 Hz with 150μm amplitude. Preindentation is 200μm; (a) is the displacement input, and (b) is the force response. For clarity, only three cycles in the sinusoidal stimulation are shown.

Figure A2.9: Stimulus and response of subject #3 at the forehead with the probe glued; Stimulation is in the tangential direction at 1 Hz with 100μm amplitude. Preindentation is 200μm; (a) is the displacement input, and (b) is the force response.

60

Figure A2.10: Stimulus and response of subject #3 at the forehead with the probe glued; Stimulation is in the tangential direction at 1 Hz with 100μm amplitude. Preindentation is 200μm; (a) is the displacement input, and (b) is the force response.

Figure A2.11: Stimulus and response of subject #3 at the forehead with the probe not glued; Stimulation is in the normal direction at 100 Hz with 150μm amplitude. Preindentation is 200μm; (a) is the displacement input, and (b) is the force response. For clarity, only three cycles in the sinusoidal stimulation are shown.
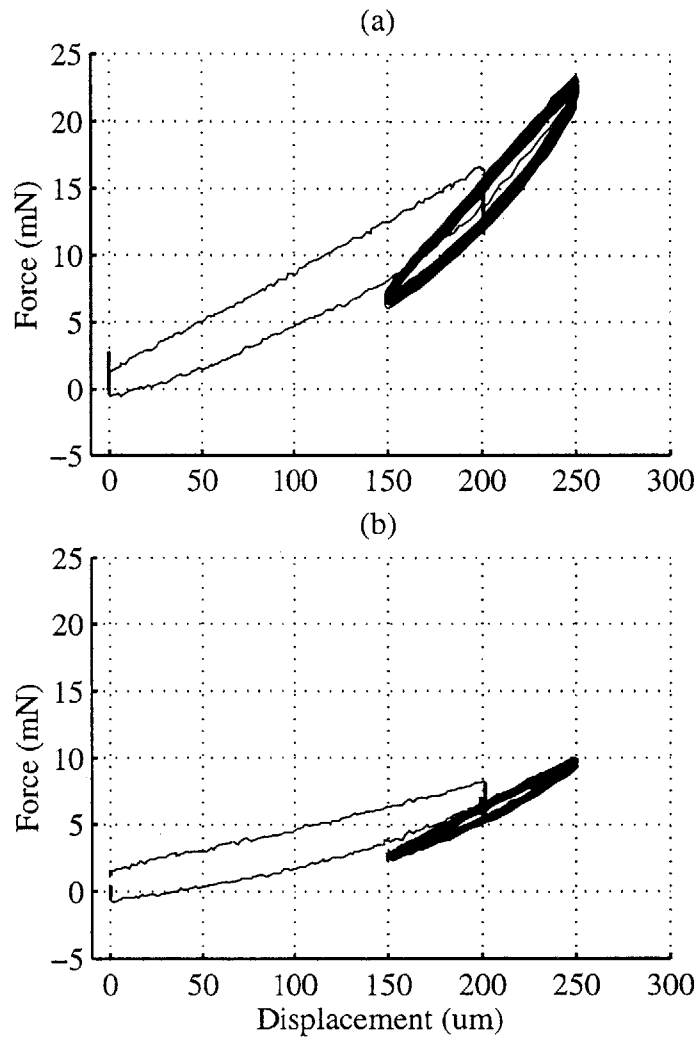
Fig. A3.1: Force v. Position for the wrist under stimulation in the normal direction at 100 Hz and 50μm amplitude with (a) the probe glued and (b) the probe not glued. Both plots show results from subject #4 under similar test conditions.
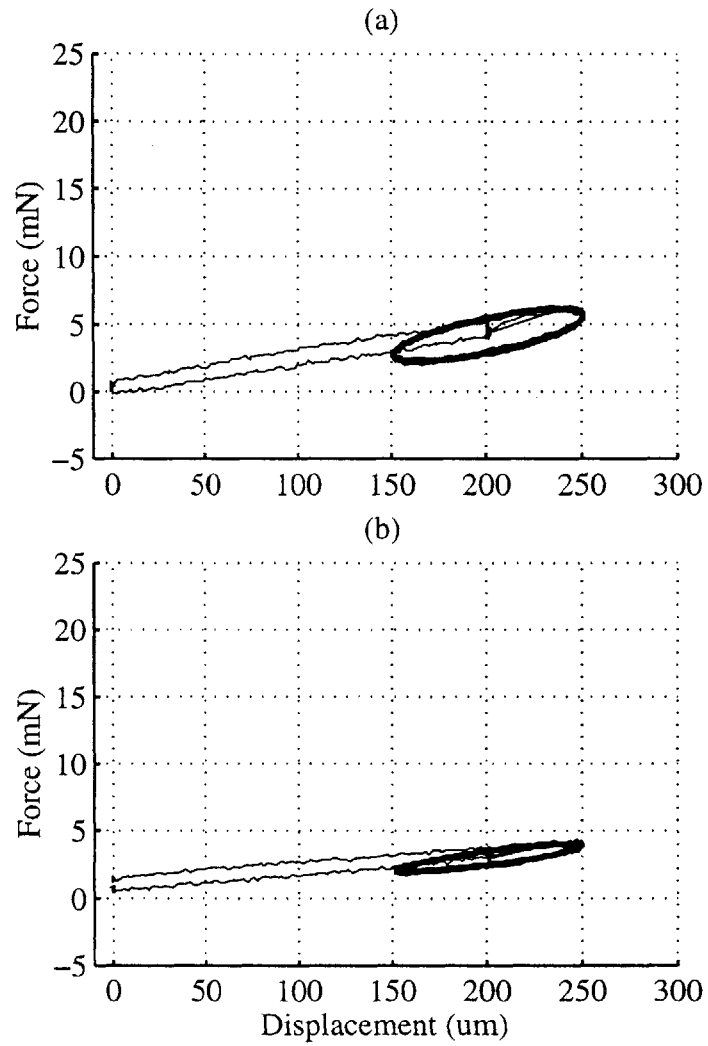
Fig. A3.2: Force v. Position for the forearm under stimulation in the normal direction at 100 Hz and 50μm amplitude with (a) the probe glued and (b) the probe not glued. Both plots show results from subject #7 under similar test conditions.
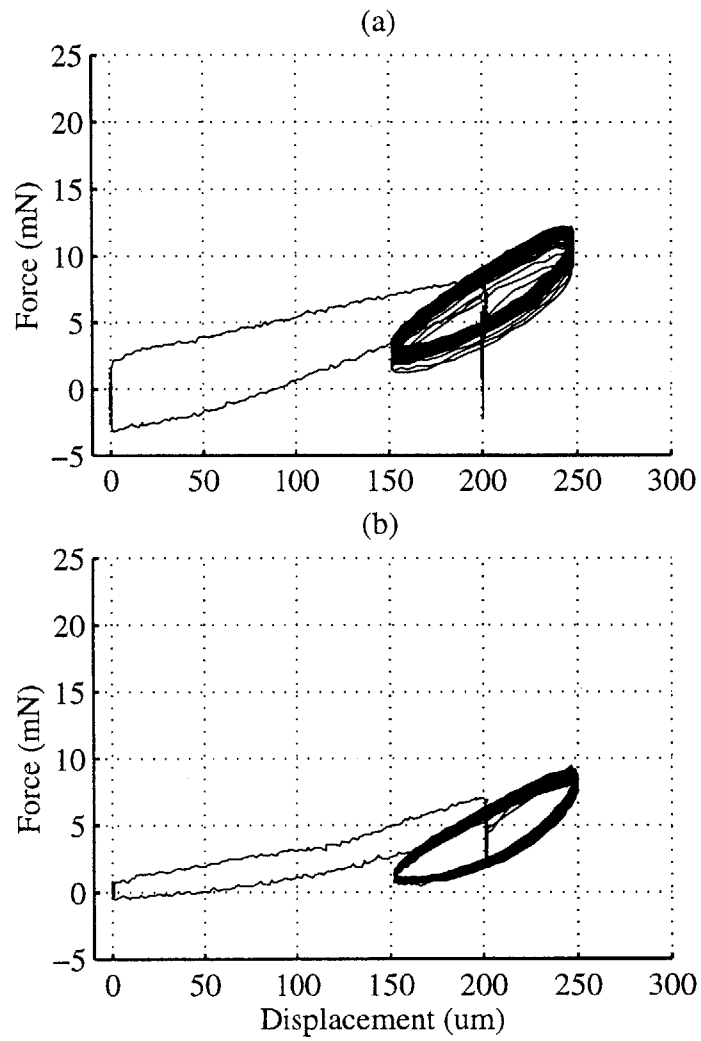
Fig. A3.3: Force v. Position for the forearm under stimulation in the normal direction at 100 Hz and 50μm amplitude with (a) the probe glued and (b) the probe not glued. Both plots show results from subject #7 under similar test conditions.
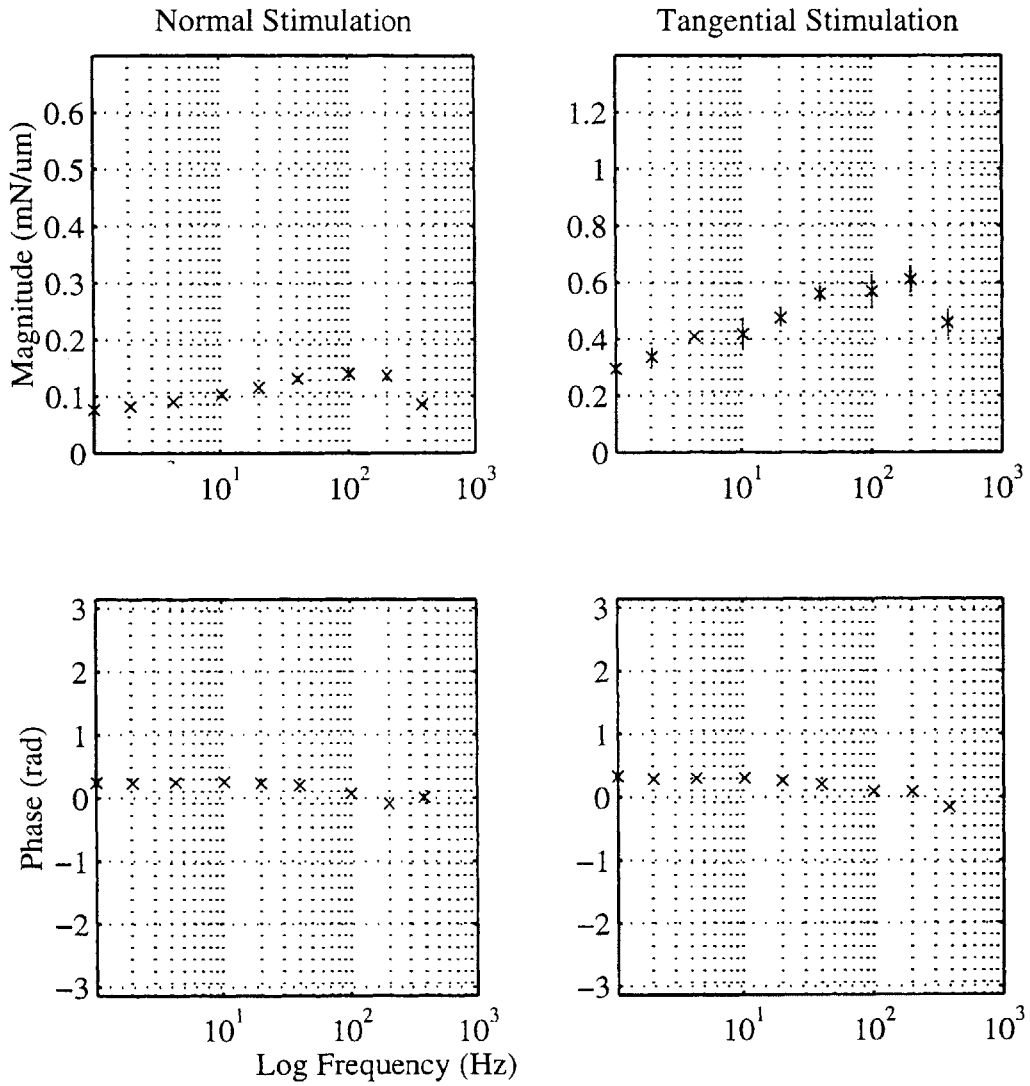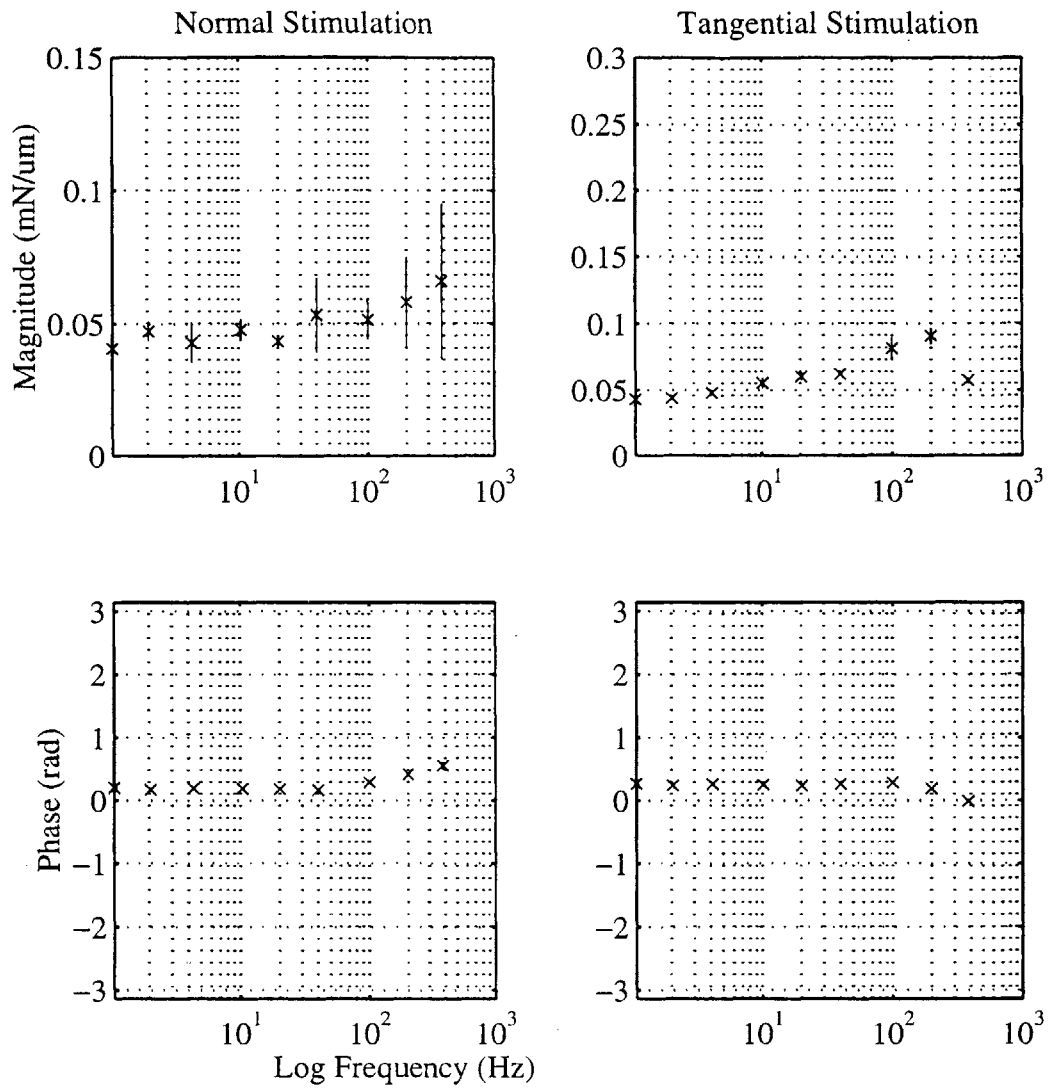
Fig. A4.1 Impedance magnitude and phase at the finger pad for normal and tangential stimulation. The plots show the impedance averaged over the repetitions at each frequency for subject #1. Error bars show standard deviation across repetitions.
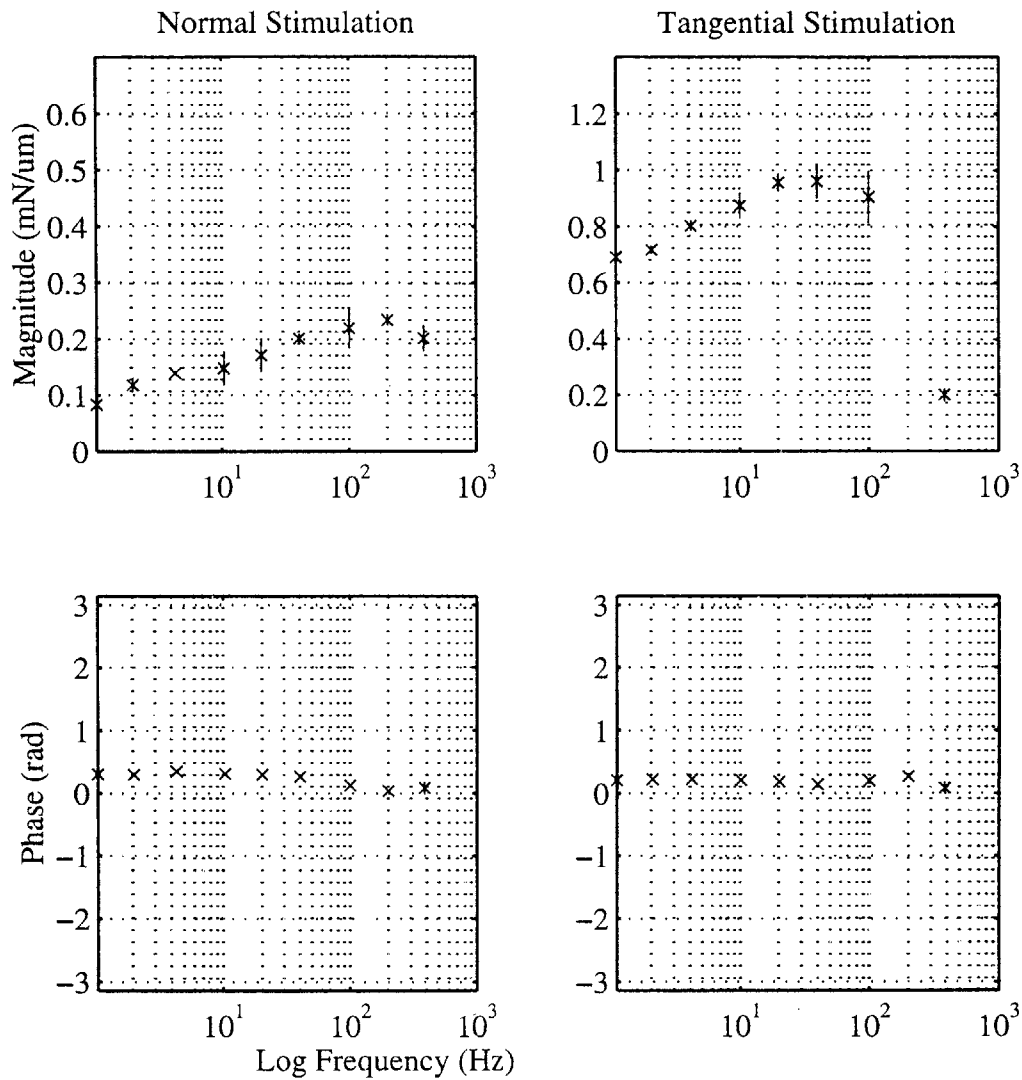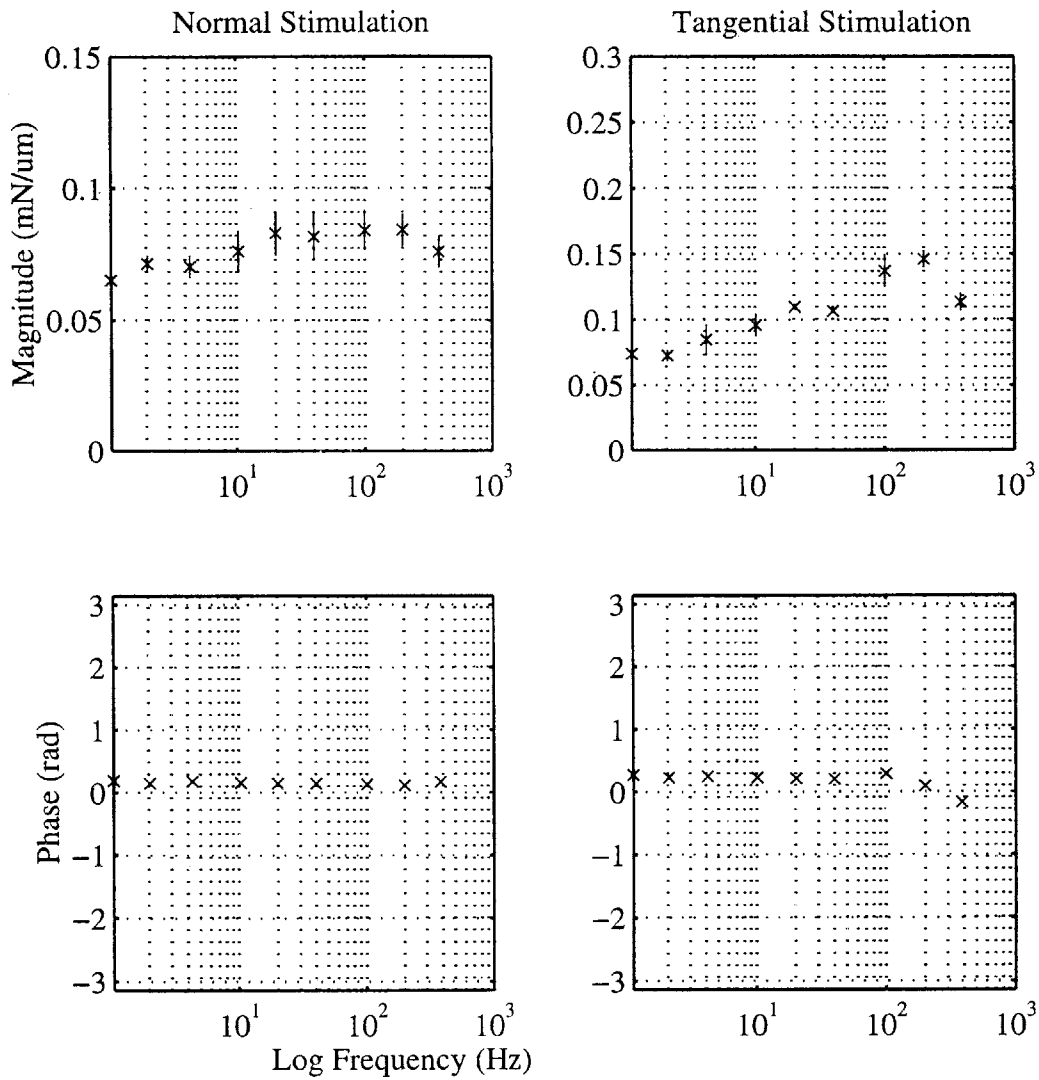
Fig. A4.2 Impedance magnitude and phase at the finger pad for normal and tangential

stimulation. The plots show the impedance averaged over the repetitions at each frequency

for subject #2. Error bars show standard deviation across repetitions.
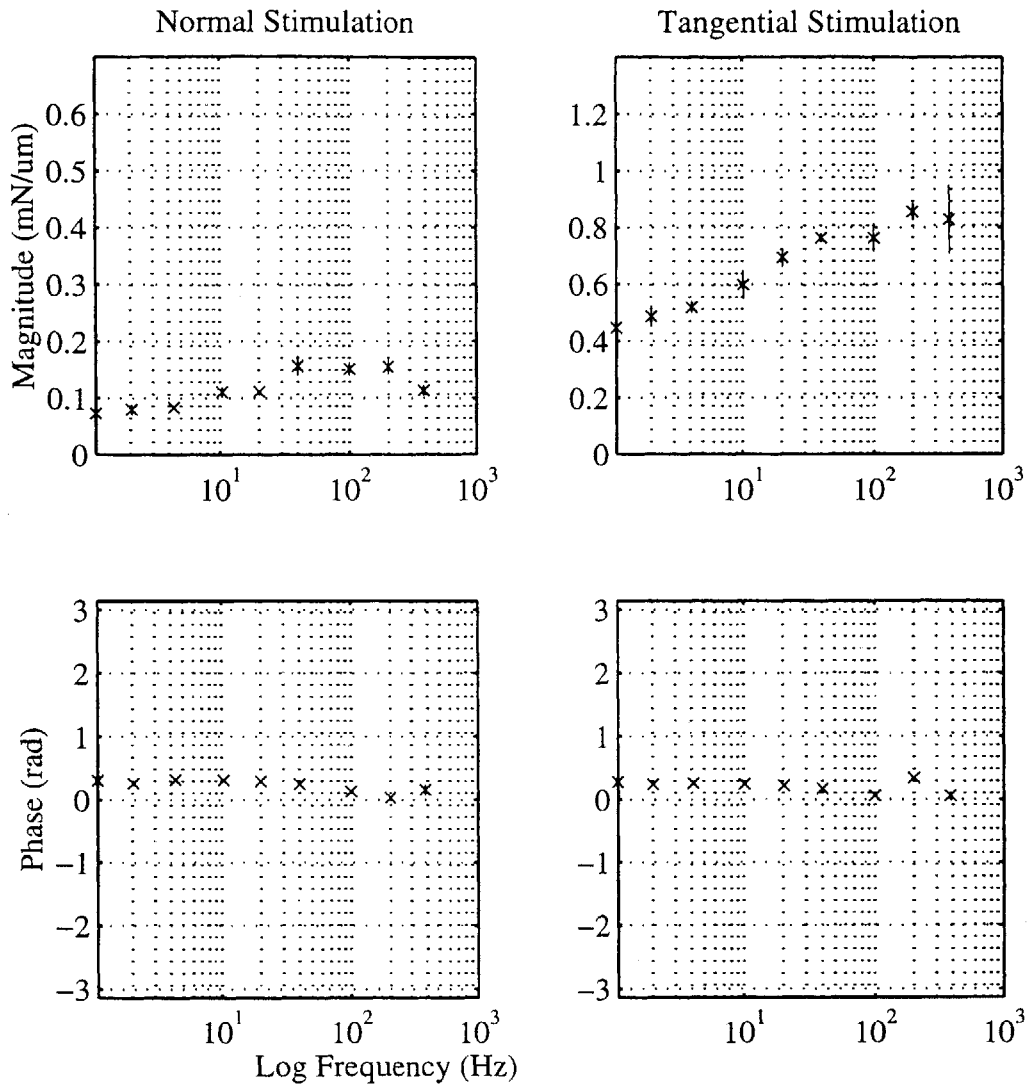
Fig. A4.3 Impedance magnitude and phase at the finger pad for normal and tangential stimulation. The plots show the impedance averaged over the repetitions at each frequency for subject #3. Error bars show standard deviation across repetitions.
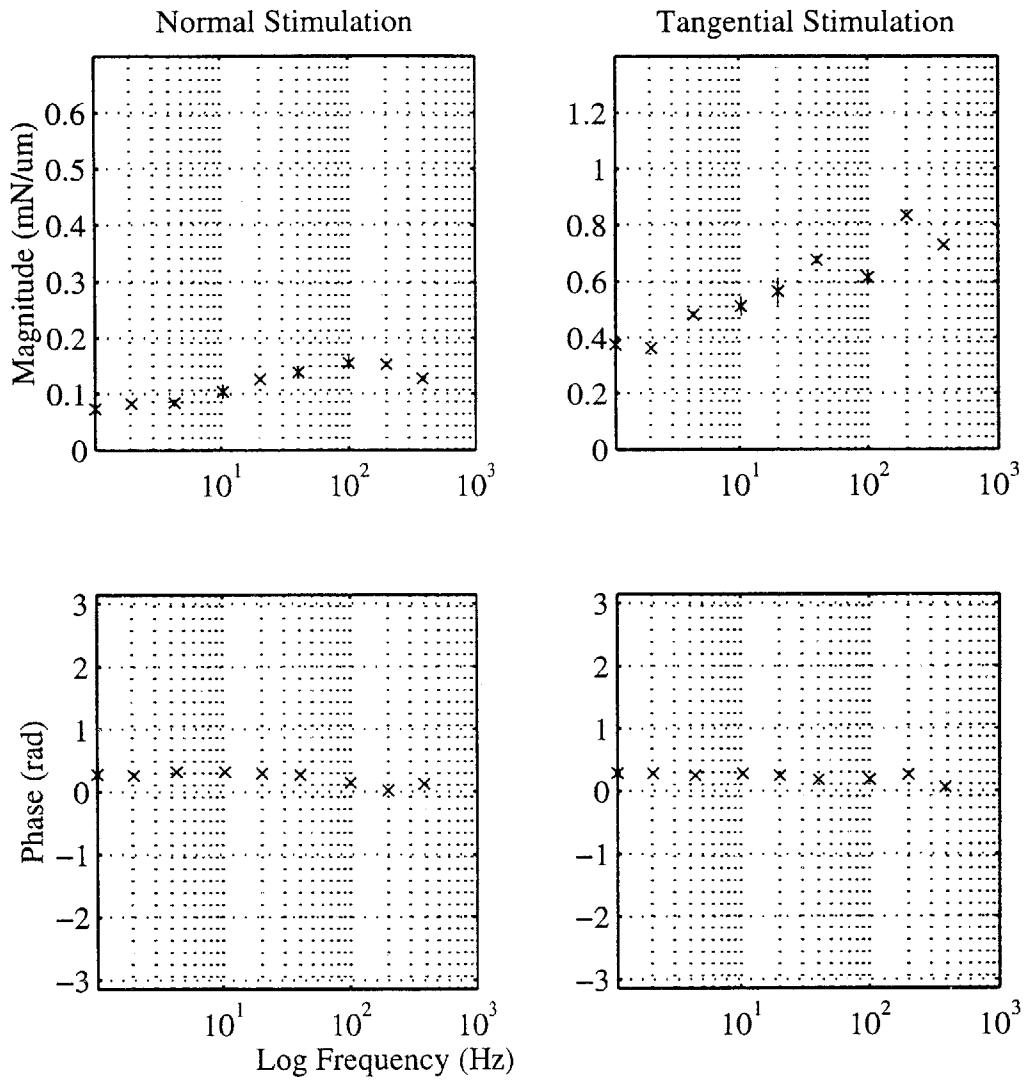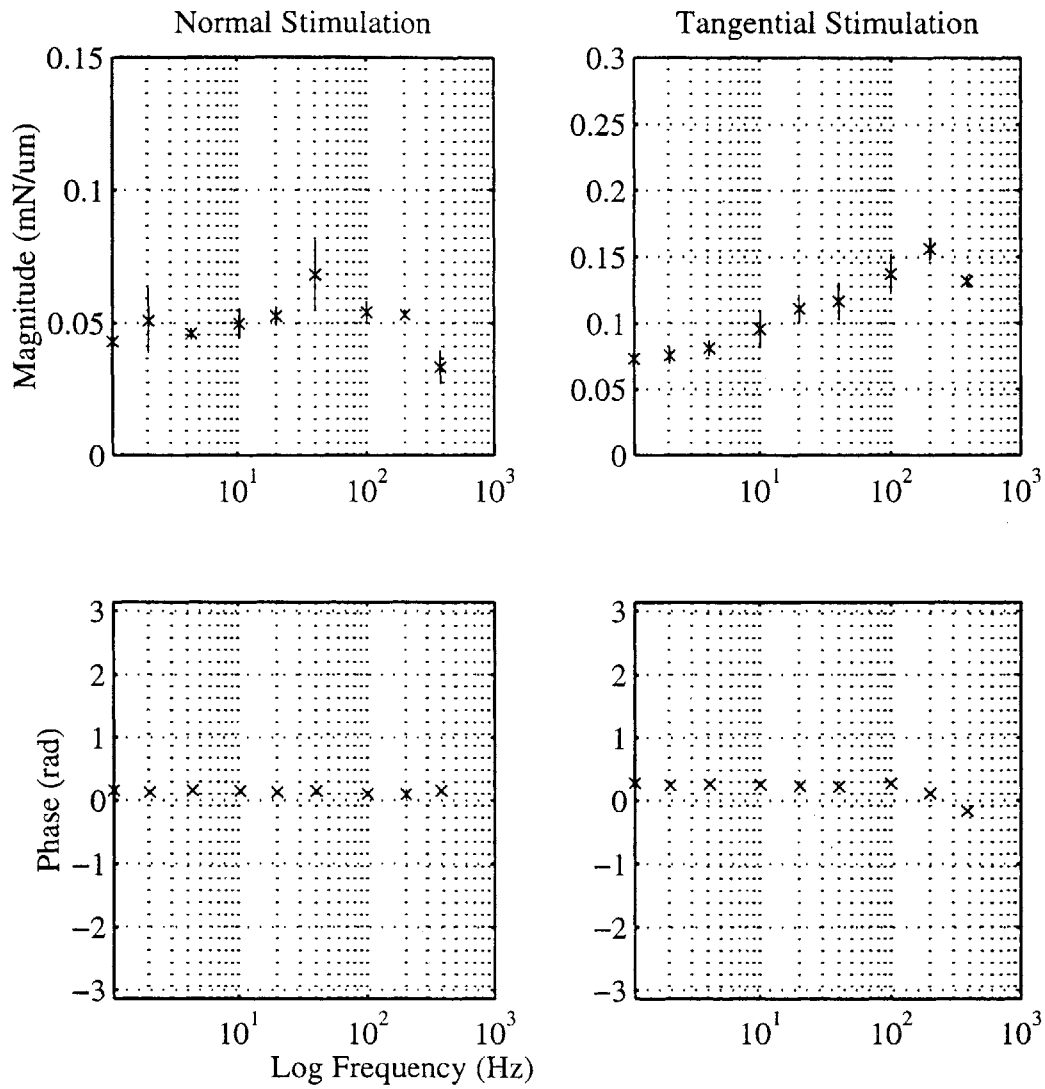
Fig. A4.4 Impedance magnitude and phase at the finger pad for normal and tangential

stimulation. The plots show the impedance averaged over the repetitions at each frequency

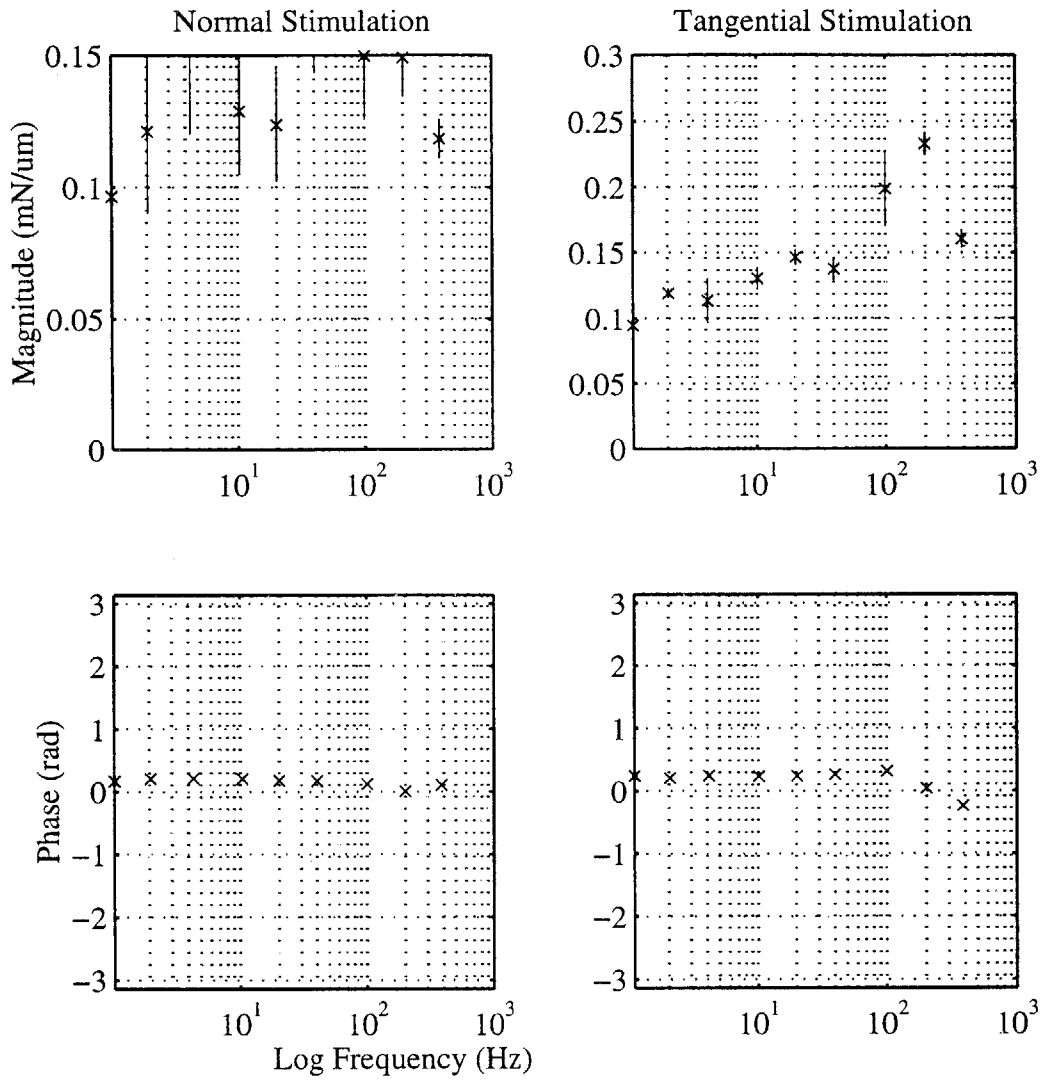for subject #4. Error bars show standard deviation across repetitions.
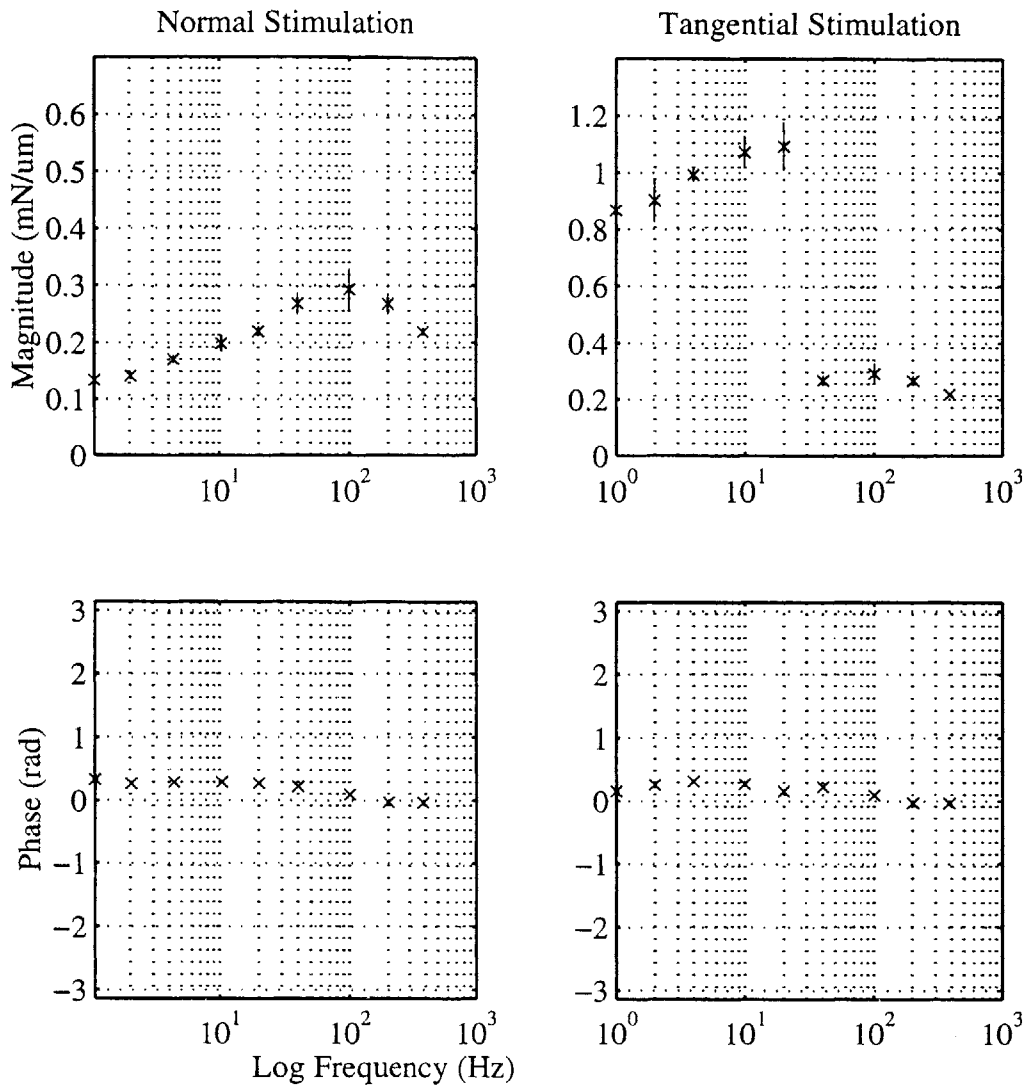
Fig. A4.5 Impedance magnitude and phase at the finger pad for normal and tangential stimulation. The plots show the impedance averaged over the repetitions at each frequency for subject #5. Error bars show standard deviation across repetitions.
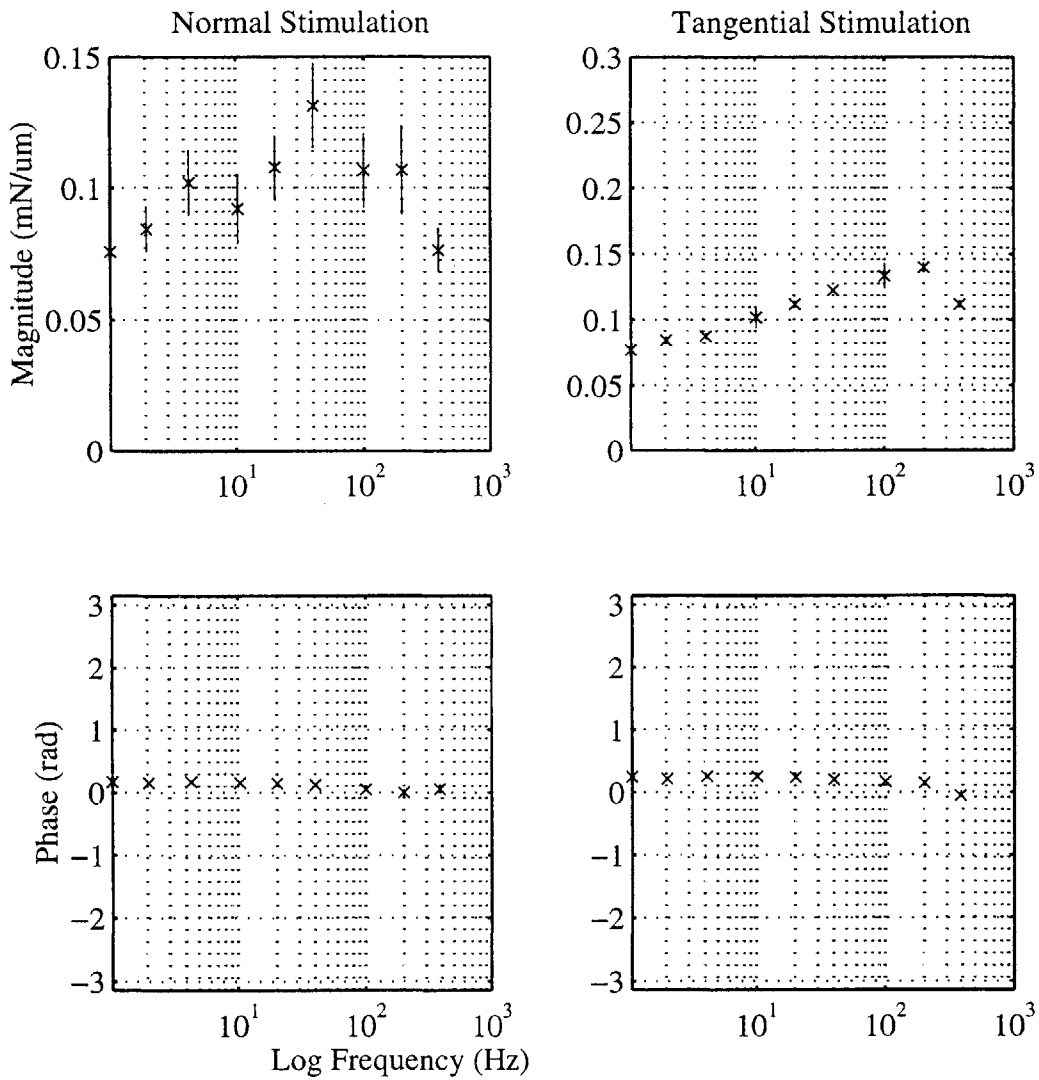
Fig. A4.6 Impedance magnitude and phase at the wrist for normal and tangential

stimulation. The plots show the impedance averaged over the repetitions at each frequency

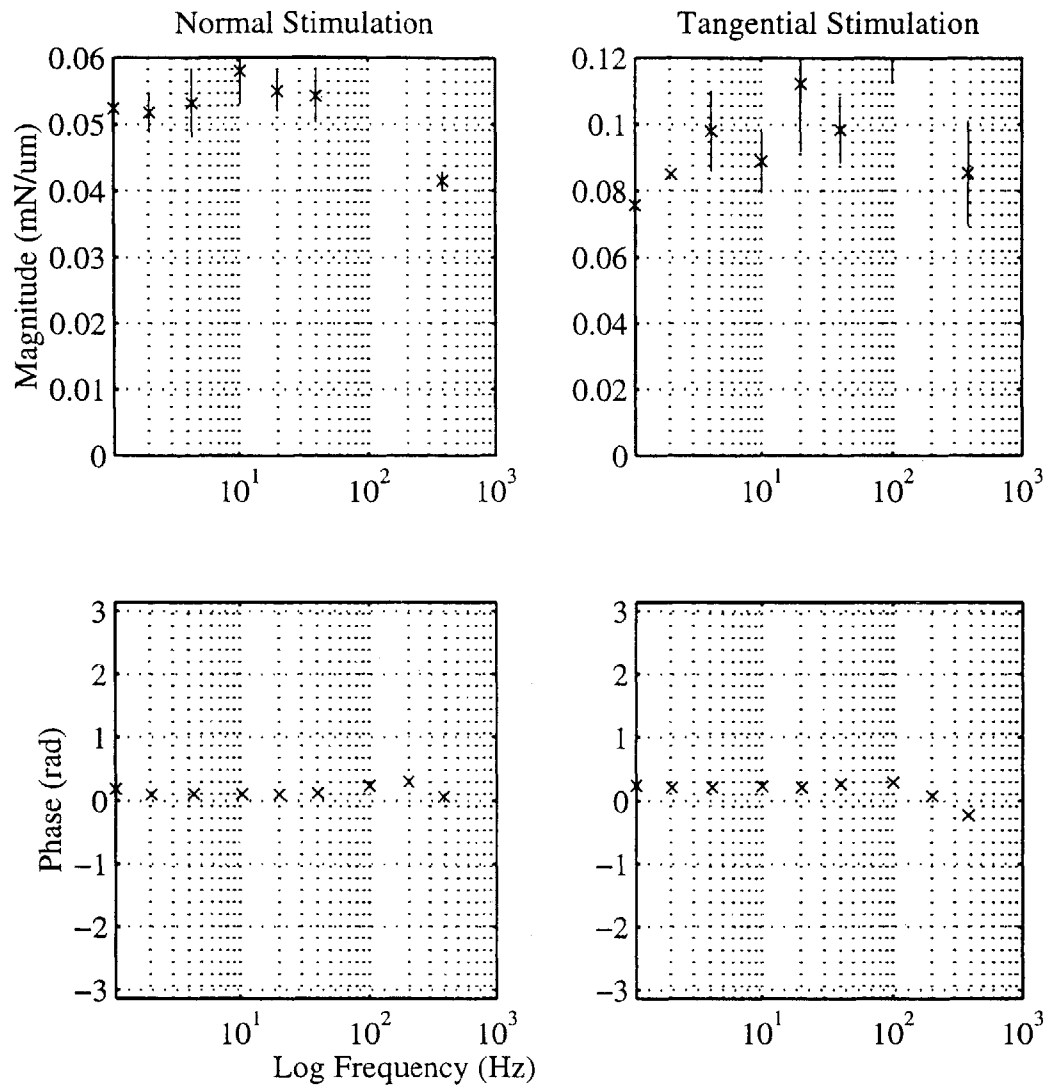for subject #6. Error bars show standard deviation across repetitions.

Fig. A4.7 Impedance magnitude and phase at the wrist for normal and tangential stimulation. The plots show the impedance averaged over the repetitions at each frequency for subject #7. Error bars show standard deviation across repetitions.
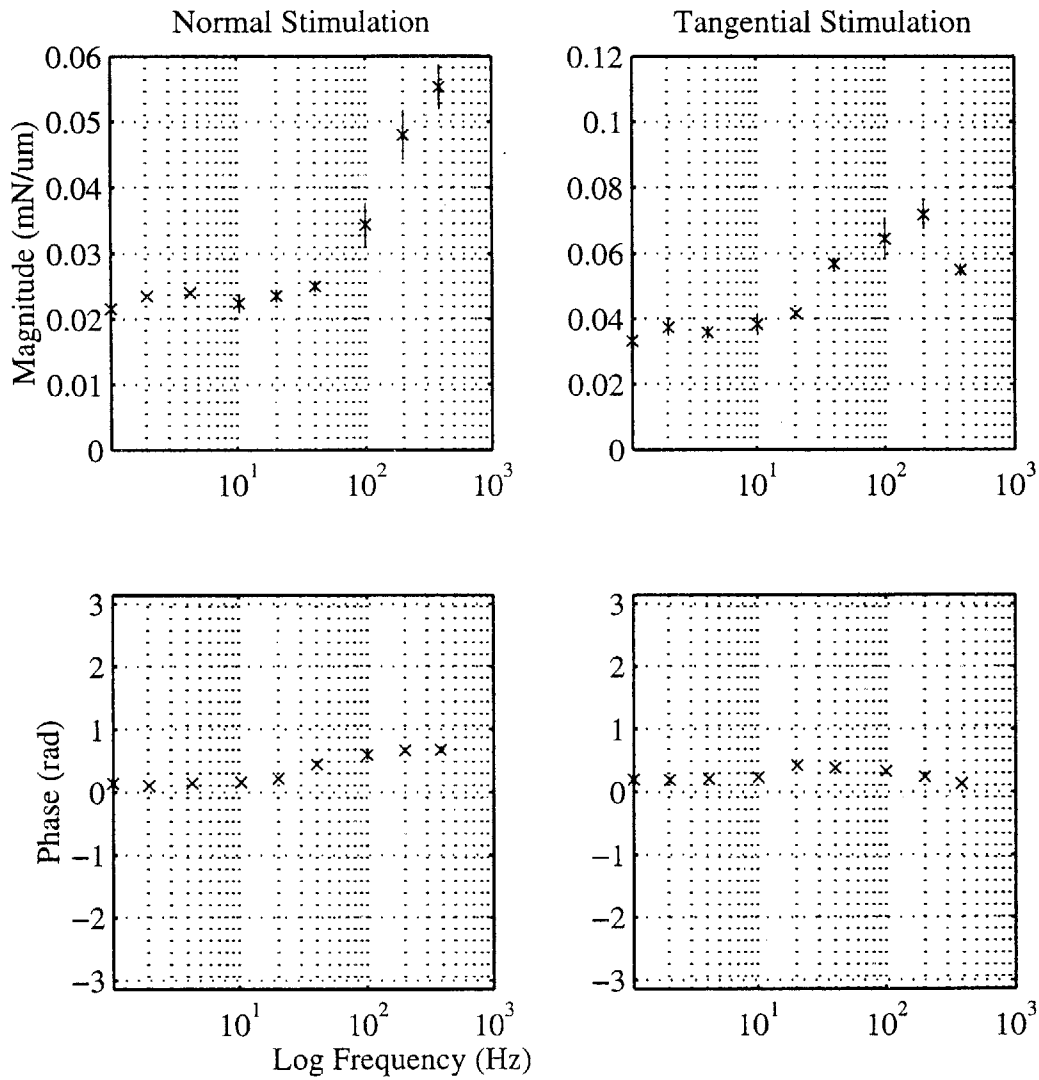
Fig. A4.8 Impedance magnitude and phase at the wrist for normal and tangential stimulation. The plots show the impedance averaged over the repetitions at each frequency for subject #3. Error bars show standard deviation across repetitions.

Fig. A4.9 Impedance magnitude and phase at the wrist for normal and tangential

stimulation. The plots show the impedance averaged over the repetitions at each frequency

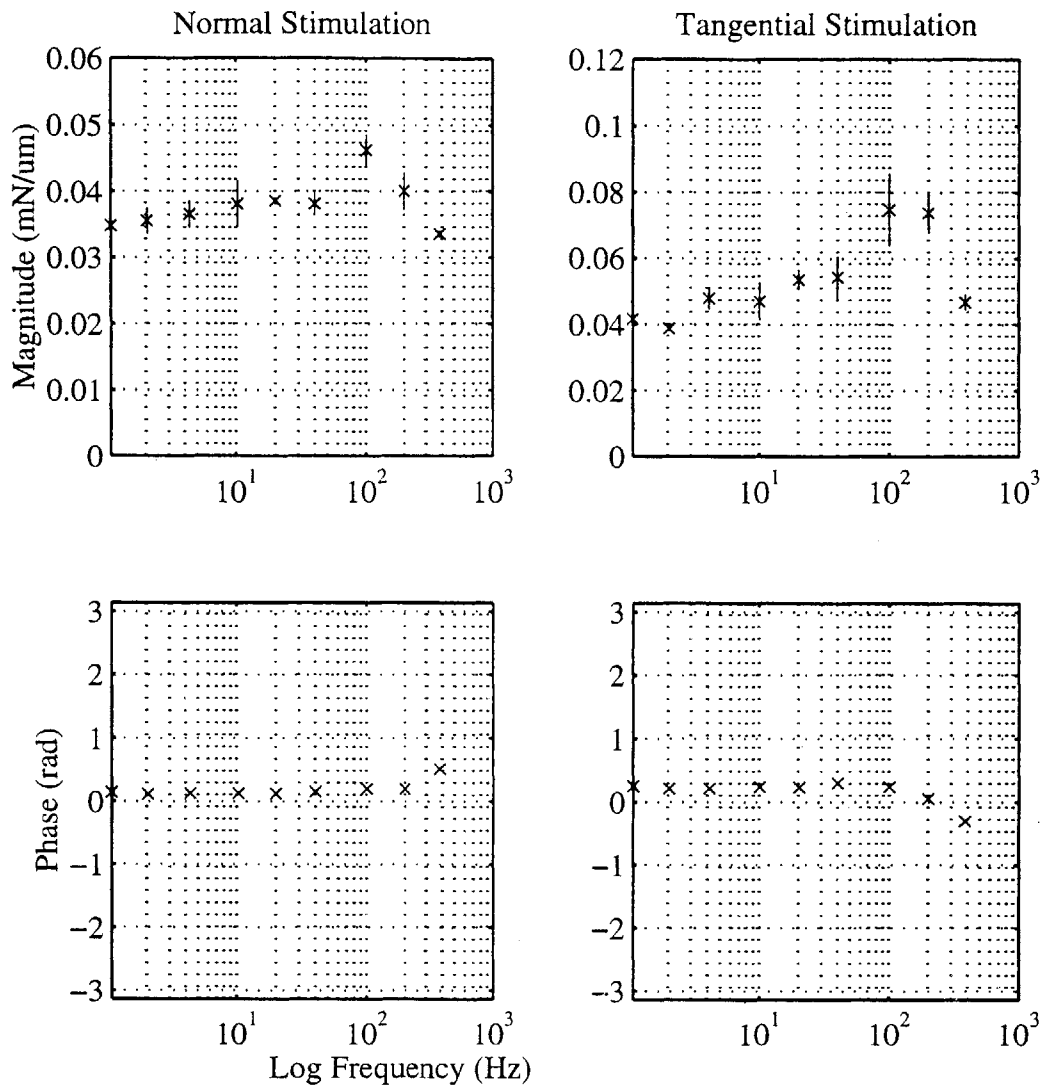for subject #5. Error bars show standard deviation across repetitions.

Fig. A4.10 Impedance magnitude and phase at the wrist for normal and tangential

stimulation. The plots show the impedance averaged over the repetitions at each frequency

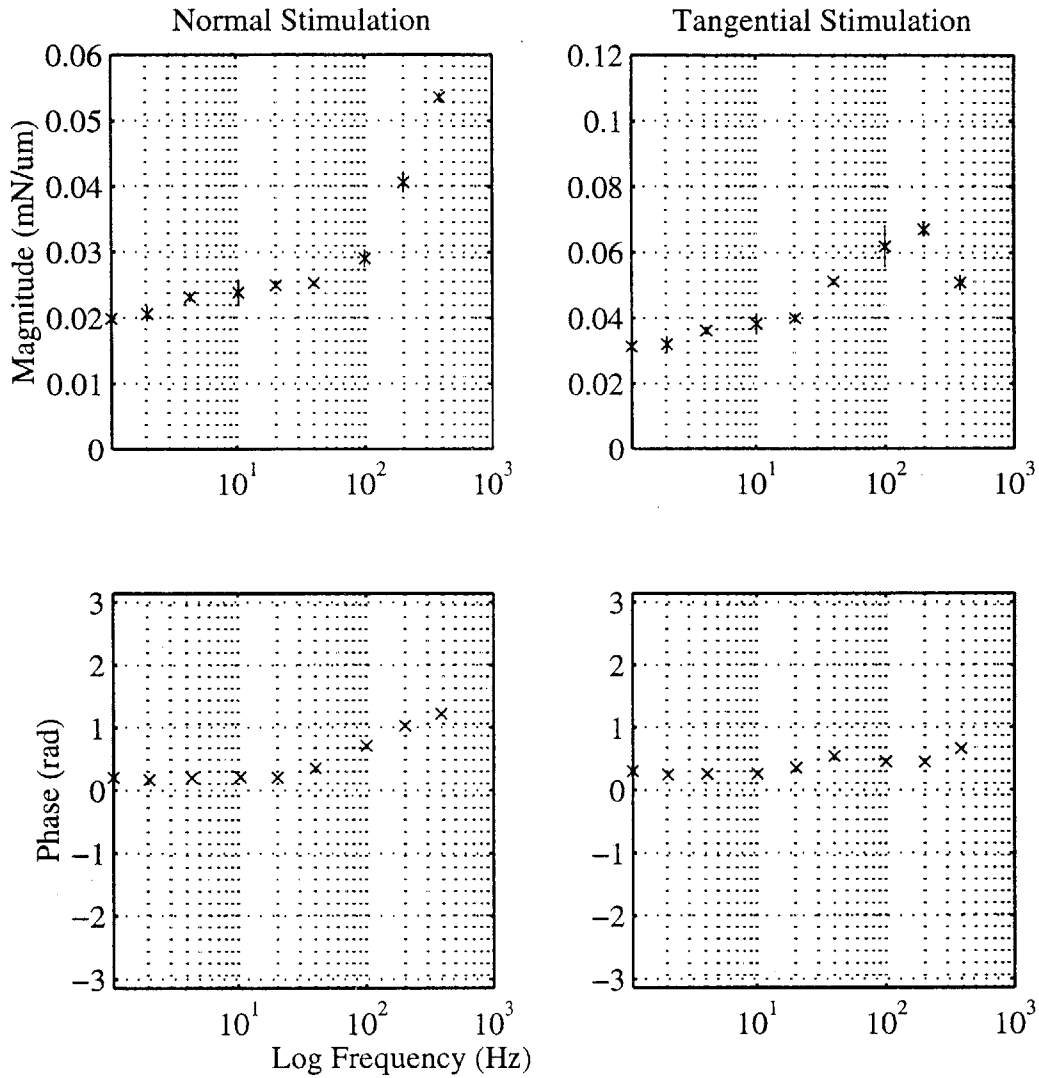for subject #4. Error bars show standard deviation across repetitions.

Fig. A4.11 Impedance magnitude and phase at the forearm for normal and tangential stimulation. The plots show the impedance averaged over the repetitions at each frequency for subject #3. Error bars show standard deviation across repetitions.
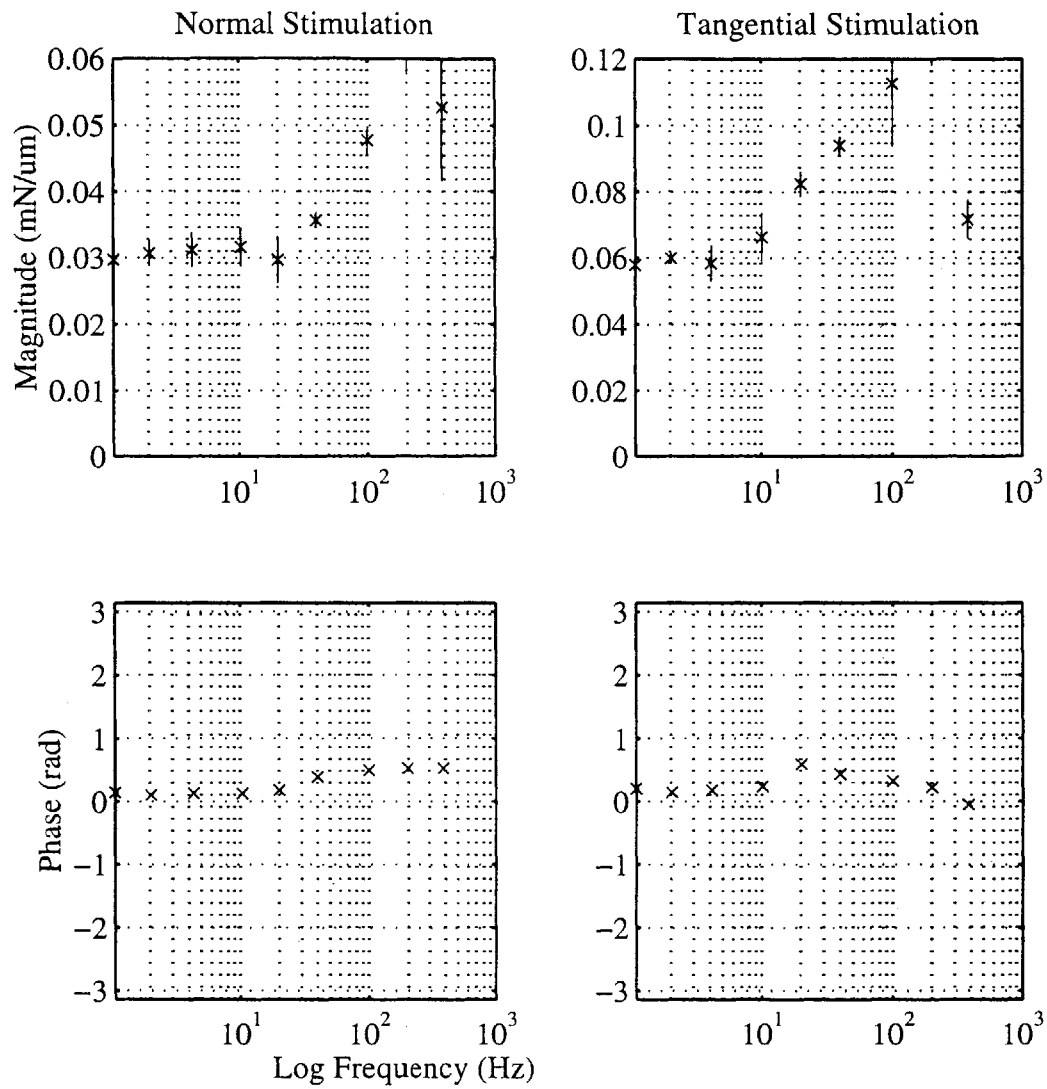
Fig. A4.12 Impedance magnitude and phase at the forearm for normal and tangential

stimulation. The plots show the impedance averaged over the repetitions at each frequency

for subject #7. Error bars show standard deviation across repetitions.

Fig. A4.13 Impedance magnitude and phase at the forearm for normal and tangential stimulation. The plots show the impedance averaged over the repetitions at each frequency for subject #5. Error bars show standard deviation across repetitions.
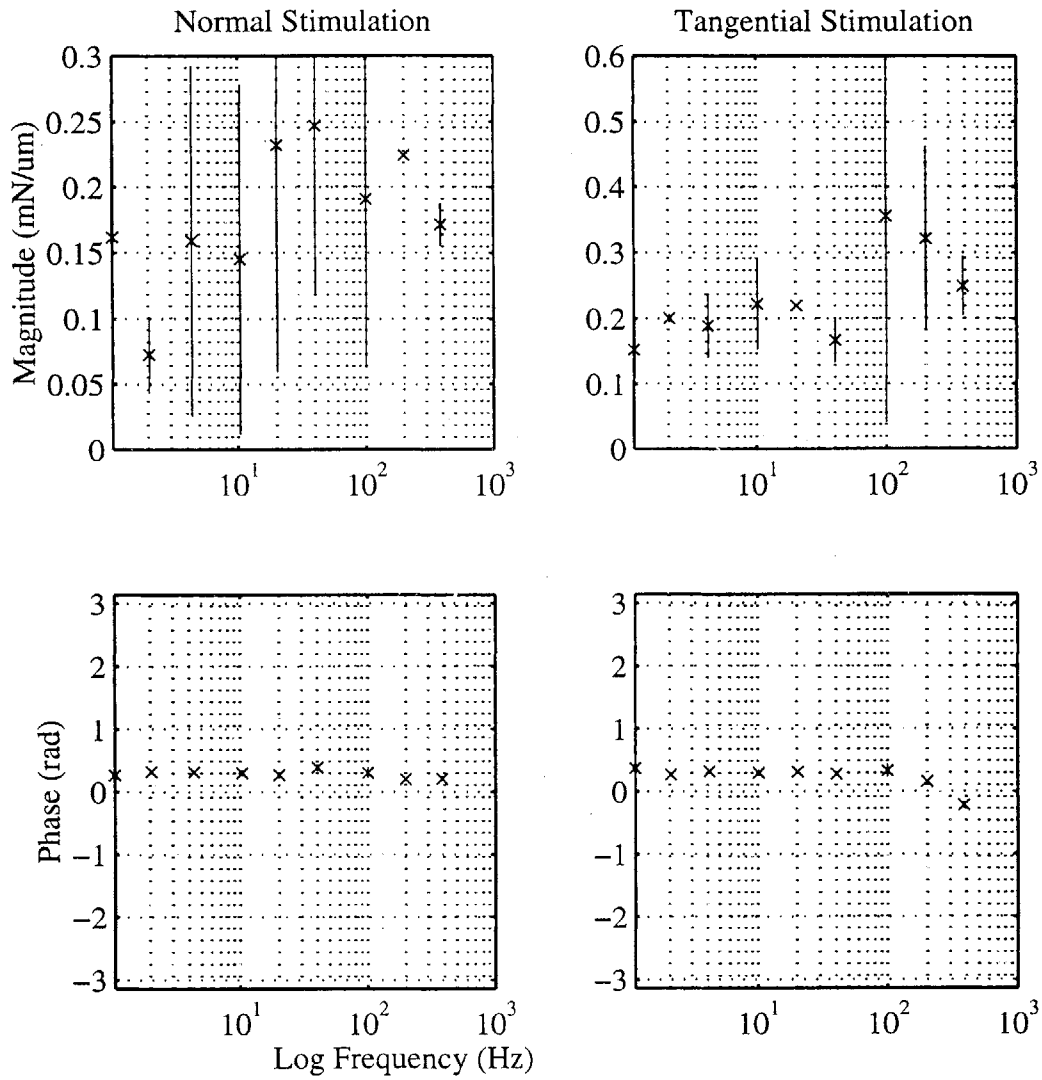
Fig. A4.14 Impedance magnitude and phase at the forearm for normal and tangential stimulation. The plots show the impedance averaged over the repetitions at each frequency for subject #8. Error bars show standard deviation across repetitions.

Fig. A4.15 Impedance magnitude and phase at the forearm for normal and tangential stimulation. The plots show the impedance averaged over the repetitions at each frequency for subject #9. Error bars show standard deviation across repetitions.
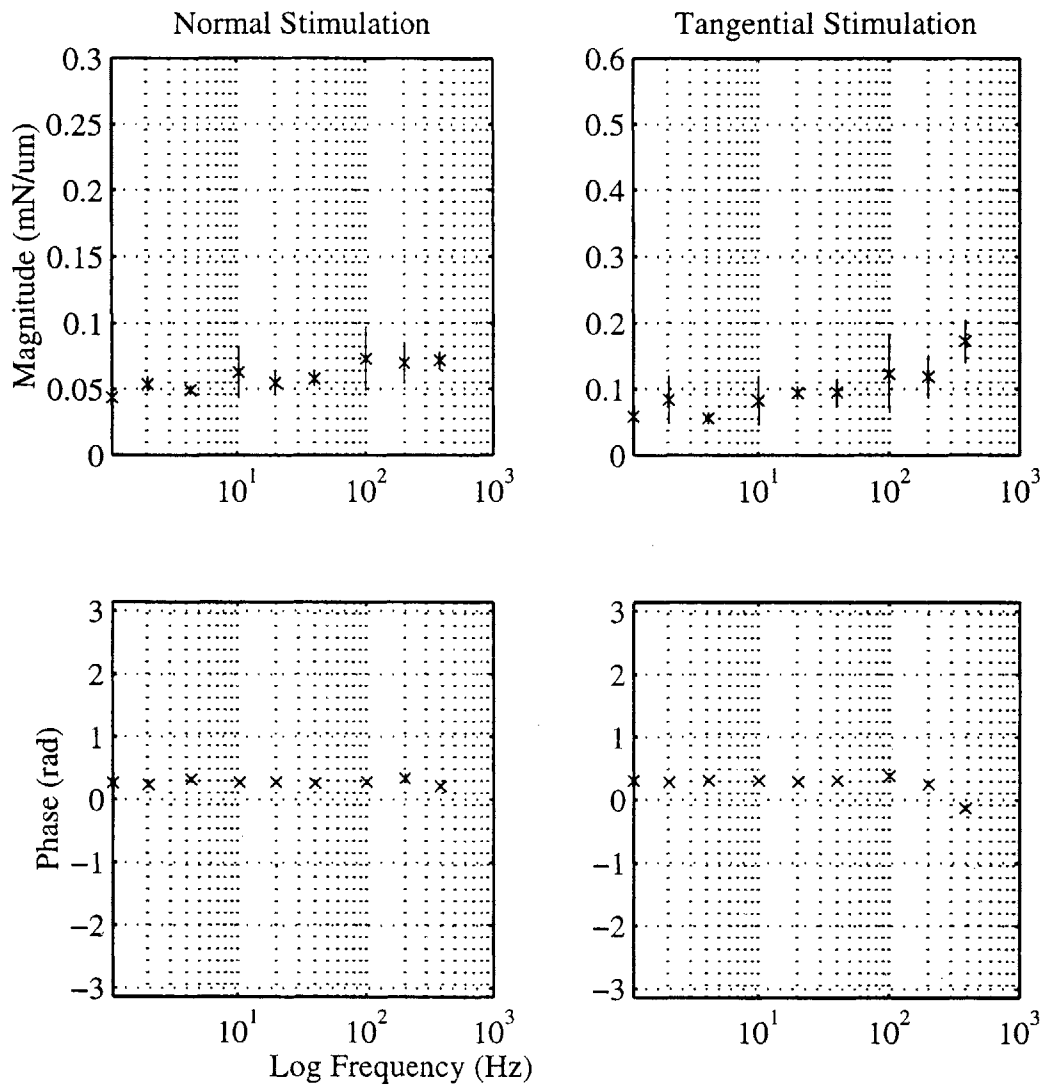
Fig. A4.16 Impedance magnitude and phase at the forehead for normal and tangential stimulation. The plots show the impedance averaged over the repetitions at each frequency for subject #7. Error bars show standard deviation across repetitions.
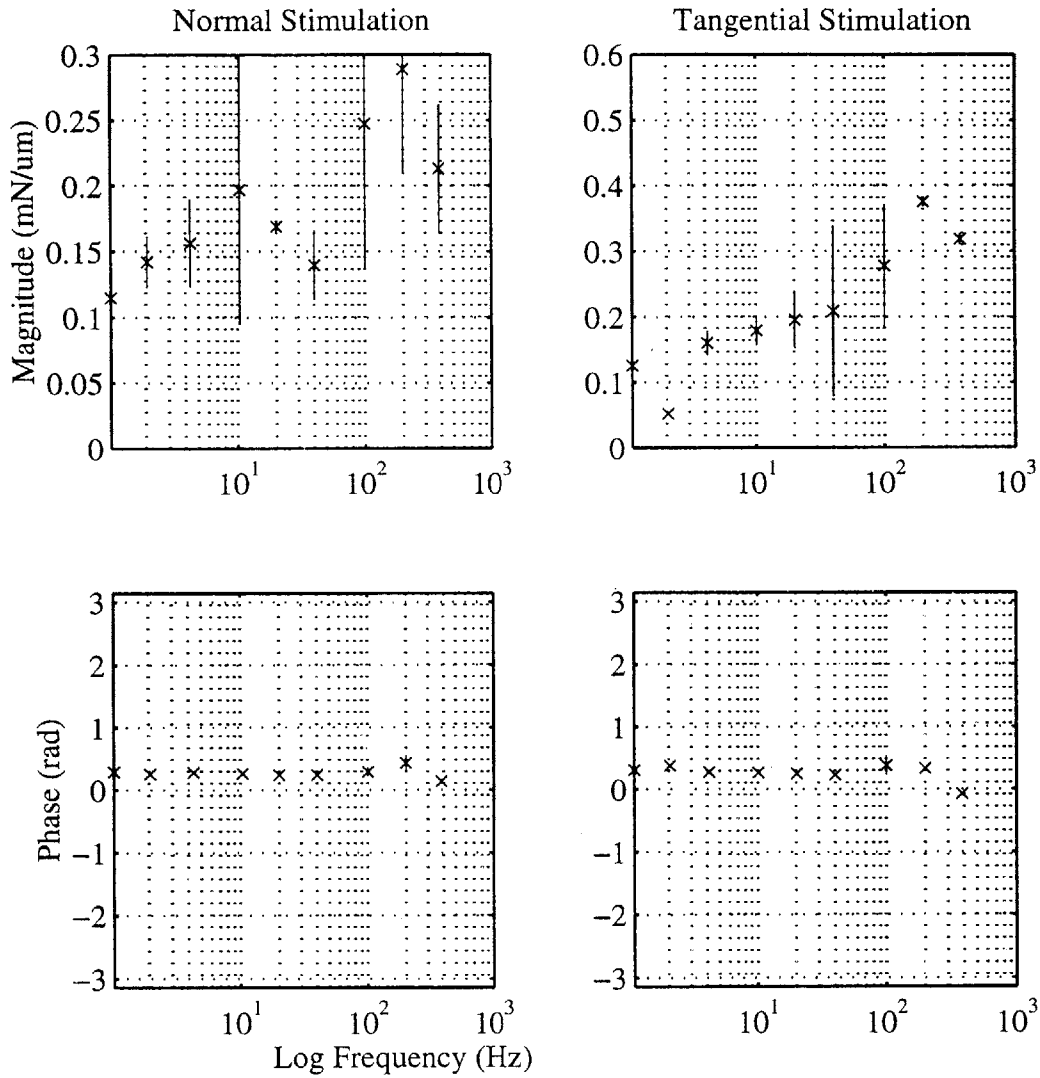
Fig. A4.17 Impedance magnitude and phase at the forehead for normal and tangential

stimulation. The plots show the impedance averaged over the repetitions at each frequency

for subject #10. Error bars show standard deviation across repetitions.

Fig. A4.18 Impedance magnitude and phase at the forehead for normal and tangential stimulation. The plots show the impedance averaged over the repetitions at each frequency for subject #3. Error bars show standard deviation across repetitions.
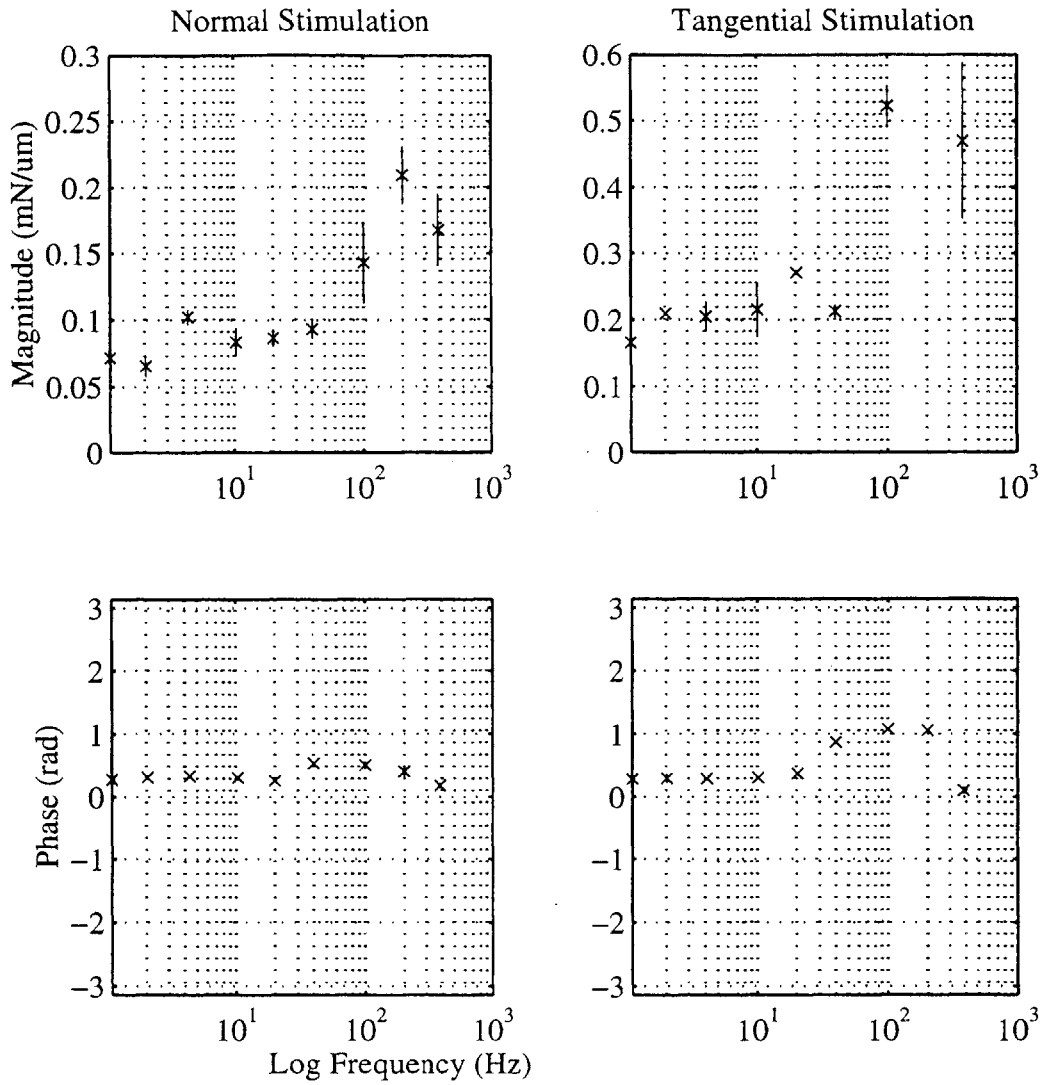
Fig. A4.19 Impedance magnitude and phase at the forehead for normal and tangential stimulation. The plots show the impedance averaged over the repetitions at each frequency for subject #11. Error bars show standard deviation across repetitions.
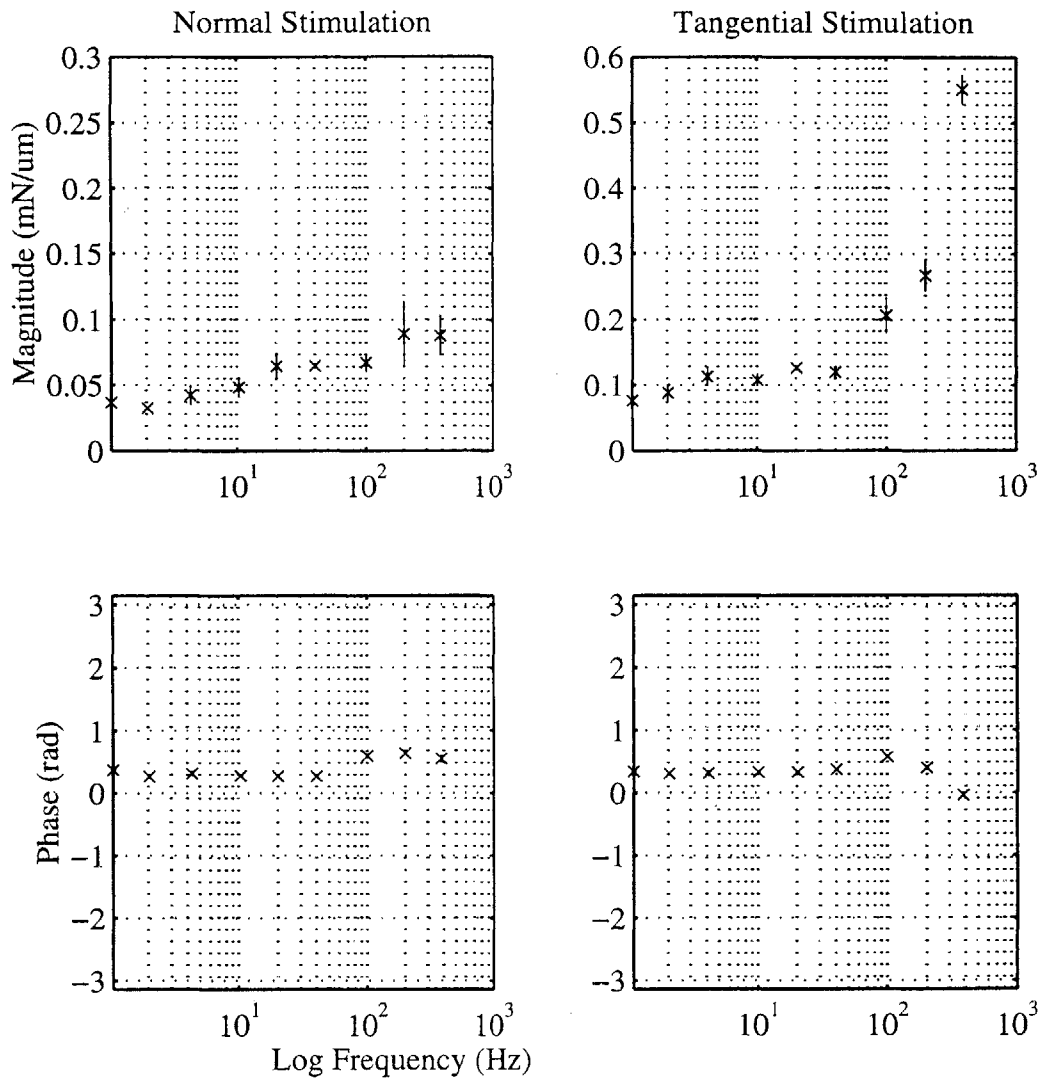
Fig. A4.20 Impedance magnitude and phase at the forehead for normal and tangential stimulation. The plots show the impedance averaged over the repetitions at each frequency for subject #12. Error bars show standard deviation across repetitions.